

# MUMUG: a fast Monte Carlo generator for radiative muon pair production (a pedagogical tutorial)

Z. K. Silagadze

Received: date / Accepted: date

**Abstract** A fast leading-order Monte Carlo generator for the process  $e^+e^- \rightarrow \mu^+\mu^-\gamma$  is described. In fact, using the  $e^+e^- \rightarrow \mu^+\mu^-\gamma$  process as an example, we provide a pedagogical demonstration of how a Monte Carlo generator can be created from scratch. The  $e^+e^- \rightarrow \mu^+\mu^-\gamma$  process was chosen, since in this case we are not faced with either too trivial or too difficult a task. Matrix elements are calculated using the helicity amplitude method. Monte Carlo algorithm uses the acceptance-rejection method with an appropriately chosen simplified distribution that can be generated using an efficient algorithm. We provide a detailed pedagogical exposition of both the helicity amplitude method and the Monte Carlo technique, which we hope will be useful for high energy physics students.

**Keywords** High energy physics; Monte Carlo simulation; Helicity amplitude method; Acceptance-Rejection Algorithm; Physics education.

## 1 introduction

Budker Institute of Nuclear Physics (Novosibirsk) is currently developing an expensive and long-term ( 10 years) project for a super charm-tau factory which will require many new accelerator technologies. To test and study these technologies at the first stage of the super charm-tau factory project, it is planned to build an inexpensive, low-energy machine called  $\mu\mu$ -tron [1]. It is so named because, in addition to purely accelerator studies, it allows solving the interesting physical problem of obtaining and studying dimuonium, the bound state of the muon and anti-muon. Dimuonium has not yet been observed experimentally by anyone, and its first observation in experiments on the  $\mu\mu$ -tron would already be a significant discovery [2,3]. However, it seems that the

---

Budker Institute of Nuclear Physics and Novosibirsk State University, Novosibirsk 630090, Russia E-mail: Z.K.Silagadze@inp.nsk.su

first physical results on the  $\mu\mu$ -tron will be studies of the reactions  $e^+e^- \rightarrow \mu^+\mu^-$  and  $e^+e^- \rightarrow \mu^+\mu^-\gamma$  near the threshold. The former process can be used for the precise measurement of the CMS energy and its spread at the  $\mu\mu$ -tron collider [4]. Several accelerator technologies studies, like the development of a muon collider, could also benefit from these measurements [5].

There are several Monte Carlo programs that generate events of the process  $e^+e^- \rightarrow \mu^+\mu^-\gamma$ . Not public event generator AFKQED (supplemented by PHOTOS [6, 7] for the description of additional undetected final state radiation photons), based on the formulas of [8] in the case of  $e^+e^- \rightarrow \mu^+\mu^-\gamma$ , was used by BABAR collaboration in their analysis of hadron production via radiative return processes [9, 10]<sup>1</sup>. PHOKHARA generator (beginning with version 4.0) [13] includes next-to-leading order radiative corrections (one-loop corrections and emission of the second real photon) to the reaction  $e^+e^- \rightarrow \mu^+\mu^-\gamma$ . While PHOKHARA is based on fixed order perturbation theory calculations, KKMC generator [14, 15] uses Yennie-Frautschi-Suura type exponentiation formula to sum leading higher order effects in initial state radiation and thus includes most of the third order leading-logarithmic contributions absent in PHOKHARA 4.0. Let us mention also MCGPJ generator [16] in which  $e^+e^- \rightarrow \mu^+\mu^-\gamma$  is implemented using formulas of [8] and the formalism of structure functions is used to incorporate the leading logarithmic contributions related to the emission of photon jets in the collinear region.

The aforementioned generators are more than enough for background studies at  $\mu\mu$ -tron. However, we decided to develop our own MUMUG generator mainly for pedagogical purposes – to teach our students how to create a Monte Carlo generator from scratch, and how to use the spinor helicity amplitudes method [17], which allows to organize the program in such a way that adding any new corrections (for example, Coulomb corrections important near the threshold [18]) becomes relatively easy. This last feature is due to the fact that in the Monte Carlo generator based on the helicity amplitude method, we calculate individual helicity amplitudes as complex numbers in the corresponding software modules. Adding new contributions (comming, for example, from the  $Z$ -boson exchange) will only require the addition of new program units to calculate these contributions, which are then added to the corresponding helicity amplitudes. At the same time, other program blocks that calculate the module square of the total amplitude and generate events based on it do not need to be changed.

At present MUMUG simulates  $e^+e^- \rightarrow \mu^+\mu^-\gamma$  process only at the leading order (LO). To be able to perform internal consistency checks, various methods is incorporated in MUMUG to obtain the tree level amplitudes needed for the Monte Carlo simulation. In addition to the internal consistency checks, MUMUG was tested against AFKQED in the BABAR energy region and good agreement has been reached.

---

<sup>1</sup> The radiative return method is of great importance for measuring the hadron cross sections [11]. It is based on the observation that for radiation in the initial state, the following factorization is exact [11, 12]:

$$\frac{d\sigma(e^+e^- \rightarrow \text{hadrons} + \gamma)(s, x)}{dx d\cos\theta} = H(x, \cos\theta) \sigma(e^+e^- \rightarrow \text{hadrons})(s(1-x)),$$

where  $x$  is the fraction of the beam energy taken by the radiative photon, and  $\theta$  is the photon emission angle with respect to the beam. Therefore, since the function  $H(x, \cos\theta)$  is known from perturbative QED, studying the reaction  $e^+e^- \rightarrow \text{hadrons} + \gamma$  will allow to extract hadronic cross sections  $\sigma(e^+e^- \rightarrow \text{hadrons})$  in a wide range of center-of-mass energies from the fixed nominal energy of the collider down to the  $e^+e^- \rightarrow \text{hadrons}$  production threshold. The only requirement is a high luminosity of the collider at nominal energy to compesate for the higher perturbative order of  $e^+e^- \rightarrow \text{hadrons} + \gamma$  compared to  $e^+e^- \rightarrow \text{hadrons}$ .

Much attention was paid to the optimization of the Monte Carlo algorithm, and thanks to this MUMUG is a very fast LO generator (at BABAR energies it was more than two orders of magnitude faster than AFKQED).

Below we give a very detailed description of the calculation of the tree-level amplitudes of  $e^+e^- \rightarrow \mu^+\mu^-\gamma$  using the spinor technique, as well as of the Monte Carlo algorithm. We hope that this description will be of pedagogical value for students studying high energy physics.

The manuscript is organized as follows. In the next section, we outline the basics of the helicity amplitude method. After a brief historical introduction, we present some of the relevant formulas for the helicity amplitude method. After explaining how all spinors can be defined in terms of an auxiliary massless spinor with negative helicity, we present identities that are useful in calculating matrix elements. Then the second important ingredient of the helicity amplitude method is discussed, namely, the convenient choice of the four-vector of photon polarization. Some spinor products, the so-called  $Z$ -functions are introduced as useful building blocks for helicity amplitudes. The developed technique is used in the next section to calculate  $e^+e^- \rightarrow \mu^+\mu^-\gamma$  tree level helicity amplitudes. The fourth section describes the Monte Carlo algorithm used in the event generator. After some general remarks about the acceptance-rejection Monte Carlo method, the rough distributions for the initial and final state radiations are presented, which are used in the acceptance-rejection algorithm. Brief concluding remarks end the article. For the convenience of readers, the appendix contains the Feynman rules used in the main text, as well as instructions for using the developed Fortran program.

## 2 Basics of the spinor technique

In this section we shall present a summary of phase conventions and other relevant formulas of the spinor technique. More details can be found in the literature [19,20,21,22] on which our presentation is based.

### 2.1 A brief historical introduction

Experimental developments in high-energy physics around the 1980s showed that the theoretical description of higher order QCD reactions, in particular, hard processes with multi-jet production, requires improved computing technology, since several hundred Feynman diagrams could not be calculated by traditional methods, even with the use of symbolic-algebraic and numerical methods [23].

The usefulness of helicity amplitudes for the calculation of multi-parton scattering in the high-energy limit was recognized already in 1966-67 in pioneering papers by Bjorken and Chen, and by Reading-Henry [23]. However, a real breakthrough in solving computational problems has been provided by the development of the CALKUL collaboration in their classical papers [19, 20,21,22] (see also other relevant references in [23,24]).

In the standard method for calculating cross sections of reactions with fermions in the initial and final states, we module square the corresponding  $S$ -matrix amplitude described by several Feynman diagrams, sum and average (if necessary) over the spin states of the participating fermions, and then compute the traces of the products of the gamma matrices.

However, when the number of particles participating in the reaction is large, the standard technique becomes impractical because the number of interfering Feynman diagrams increases rapidly.

One of the alternative methods that make calculations manageable in this case is the helicity amplitude method. In this method, the individual amplitudes that correspond to the scattering of the helicity eigenstates are calculated analytically as a complex number depending on the Lorentz scalars composed of the four-momenta of the participating particles. Since different helicity configurations do not interfere, knowing the individual helicity amplitudes is sufficient to calculate the module square of the  $S$ -matrix amplitude by summing the modular squares of all contributing helicity amplitudes, and these calculations can be performed numerically on a computer.

In fact, it is natural to use two-component Weyl-van der Waerden spinors in the helicity amplitude method, and a brief historical overview of the use of spinor techniques with the relevant literature can be found in [24].

In this article we use the original variant of the helicity amplitude method, as developed by the CALKUL collaboration [17, 19, 20, 21, 22]. This technique turned out to be extremely useful for QED calculations with massless fermions. However, its use in non-abelian theories such as QCD required further refinements described in the review articles [25, 26]. Using the idea that on-shell one-loop amplitudes can be reconstructed from their unitarity cuts, the use of the helicity amplitude technique can also be extended to one-loop QCD calculations [27, 28]. However, these important developments are beyond the scope of the present article.

In the next subsection we describe how both massless and massive spinors can be represented in terms of one auxiliary negative-helicity massless spinor. In this way all spinor products are expressed in terms of two types of basic spinor inner products.

After providing some usefull spinor identities, we use gauge invariance of QED to express the photon polarization four-vector in terms of a lightlike four-vector not collinear to the photon four-momentum or to the four-momentum of the auxiliary negative-helicity massless spinor mentioned previously. In specific calculations, a judicious choice of this auxiliary four-vector nulifies some Feynman diagrams and thus simplifies the calculation.

When massive spinors are involved, as in the case of  $e^+e^- \rightarrow \mu^+\mu^-\gamma$ , for a numerical evaluation it is convenient to express the helicity amplitudes in terms of the so-called  $Z$ -functions, which we discuss in the last subsection.

## 2.2 Massless and massive spinors

All spinors are determined using an auxiliary negative-helicity massless spinor  $u_-(\xi)$  with a lightlike four-momentum  $\xi$ . The conditions determining  $u_-(\xi)$  are as follows:

$$\hat{\xi}u_-(\xi) = 0, \quad \omega_-u_-(\xi) = u_-(\xi), \quad \omega_\lambda = \frac{1}{2}(1 + \lambda\gamma_5), \quad \lambda = \pm 1, \quad (1)$$

and its normalization condition is  $u_-(\xi)\bar{u}_-(\xi) = \omega_- \hat{\xi}$  (we use conventions for the space-time metric etc. accepted in the modern QFT textbooks [29]. In particular,  $\hat{\xi} = \xi_\mu \gamma^\mu$ ).

Under space inversion  $u_-(\xi) \rightarrow \gamma_0 u_-(\xi) \sim u_+(\xi')$ , where  $\xi' = (\xi_0, -\vec{\xi})$  and  $\sim$  means equality up to a phase. Let  $\eta = (0, \vec{n})$ ,  $\vec{n}^2 = 1$  and  $\vec{n} \cdot \vec{\xi} = 0$ . Then  $\hat{R}_{\vec{n}}(\pi)\xi' = \xi$ , where  $\hat{R}_{\vec{n}}(\phi)$  stands for a rotation by the angle  $\phi$  around the axis  $\vec{n}$ . Therefore  $\hat{R}_{\vec{n}}(\pi)\gamma_0 u_-(\xi) \sim u_+(\xi)$ . But

$$\hat{R}_{\vec{n}}(\pi)\gamma_0 u_-(\xi) = \exp\left(-i\frac{\pi}{2} \vec{n} \cdot \vec{\Sigma}\right)\gamma_0 u_-(\xi) = -i\vec{n} \cdot \vec{\Sigma} \gamma_0 u_-(\xi),$$

and  $-i\vec{n} \cdot \vec{\Sigma} \gamma_0 u_-(\xi) = i\vec{n} \cdot \vec{\Sigma} \gamma_0 \gamma_5 u_-(\xi)$ . For gamma matrices we use chiral representation

$$\gamma_0 = \begin{pmatrix} 0 & 1 \\ 1 & 0 \end{pmatrix}, \quad \gamma^k = \begin{pmatrix} 0 & -\sigma_k \\ \sigma_k & 0 \end{pmatrix}, \quad \gamma_5 = \begin{pmatrix} 1 & 0 \\ 0 & -1 \end{pmatrix}, \quad \Sigma^k = \begin{pmatrix} \sigma_k & 0 \\ 0 & \sigma_k \end{pmatrix},$$

so it can be checked easily that  $\Sigma^k \gamma_0 \gamma_5 = \gamma^k$ . Therefore  $u_+(\xi) \sim i n^k \gamma^k u_-(\xi) = -i \hat{\eta} u_-(\xi)$ . As was already mentioned, this relation determines the positive-helicity massless spinor  $u_+(\xi)$  only up to a phase, and the phase is fixed by the following Kleiss-Stirling convention [19]

$$u_+(\xi) = \hat{\eta} u_-(\xi), \quad \eta^2 = -1, \quad \eta \cdot \xi = 0. \quad (2)$$

It should be mentioned that the modern literature [25,26] uses a slightly different way of introducing the basic massless spinors and the associated phase convention.

Now let us construct a general massive spinor with four-momentum  $p$  ( $p^2 = m^2$ ) which besides the Dirac equation  $(\hat{p} - m)u_\lambda(p) = 0$  satisfies the normalization condition

$$u_\lambda(p) \bar{u}_\lambda(p) = \frac{1}{2}(1 + \lambda \gamma_5 \hat{s})(\hat{p} + m),$$

where  $s$  is the spin quantization vector with properties  $s^2 = -1$ ,  $s \cdot p = 0$ . This can be done by noting that

$$\begin{aligned} (\hat{p} + m)u_\lambda(\xi) &= [u_\lambda(p) \bar{u}_\lambda(p) + u_{-\lambda}(p) \bar{u}_{-\lambda}(p)] u_\lambda(\xi) = \\ &= [\bar{u}_\lambda(p) u_\lambda(\xi)] u_\lambda(p) + [\bar{u}_{-\lambda}(p) u_\lambda(\xi)] u_{-\lambda}(p). \end{aligned} \quad (3)$$

Now

$$|\bar{u}_\lambda(p) u_\lambda(\xi)|^2 = Sp \left\{ \frac{1}{2}(1 + \lambda \gamma_5 \hat{s})(\hat{p} + m) \omega_\lambda \hat{\xi} \right\} = p \cdot \xi - ms \cdot \xi. \quad (4)$$

Analogously

$$|\bar{u}_{-\lambda}(p) u_\lambda(\xi)|^2 = p \cdot \xi + ms \cdot \xi. \quad (5)$$

But  $(p - ms)^2 = 0$ , so we may try  $p - ms = k\xi$  and then  $p \cdot s = 0$  determines the coefficient  $k = m^2/p \cdot \xi$ . Therefore the following choice is a valid spin quantization vector:

$$s = \frac{p}{m} - \frac{m}{p \cdot \xi} \xi.$$

With this spin quantization vector  $ms \cdot \xi = p \cdot \xi$  and we get from (3) (the phase is again fixed according to Kleiss-Stirling [19])

$$u_\lambda(p) = \frac{(\hat{p} + m)u_{-\lambda}(\xi)}{\sqrt{2p \cdot \xi}}. \quad (6)$$

For the antiparticle spinor we have  $(\hat{p} + m)v_\lambda(p) = 0$ ,  $v_\lambda(p)\hat{v}_\lambda(p) = \frac{1}{2}(1 + \lambda \gamma_5 \hat{s})(\hat{p} - m)$ . So it can be derived in the same way as the u-type spinor above but by the change  $m \rightarrow -m$ . Note that (3), (4) and (5) indicate that one should also change  $\lambda \rightarrow -\lambda$ . Therefore a general antiparticle spinor is

$$v_\lambda(p) = \frac{(\hat{p} - m)u_\lambda(\xi)}{\sqrt{2p \cdot \xi}}. \quad (7)$$

Note that

$$\frac{\hat{p}u_{-\lambda}(\xi)}{\sqrt{2p \cdot \xi}} = \frac{\hat{p}_\xi u_{-\lambda}(\xi)}{\sqrt{2p_\xi \cdot \xi}} = u_\lambda(p_\xi),$$

where  $p_\xi$  is the lightlike four-vector:

$$p_\xi = p - \frac{m^2}{2p \cdot \xi} \xi, \quad p_\xi^2 = 0.$$

Therefore the massive spinors can always be decomposed in terms of massless spinors as follows

$$u_\lambda(p) = u_\lambda(p_\xi) + \frac{m}{\sqrt{2p \cdot \xi}} u_{-\lambda}(\xi), \quad v_\lambda(p) = u_{-\lambda}(p_\xi) - \frac{m}{\sqrt{2p \cdot \xi}} u_\lambda(\xi). \quad (8)$$

### 2.3 Useful spinor identities

In QCD calculations, the amplitudes have a large number of momenta, and for massless spinors it is useful to use the shorthand notation [25, 26, 21] (not to be confused with Dirac's bra-ket notation for quantum state vectors)

$$\begin{aligned} u_-(\xi) &= |\xi] \equiv |\xi - \rangle, & u_+(\xi) &= |\xi\rangle \equiv |\xi + \rangle, \\ \bar{u}_-(\xi) &= \langle \xi| \equiv \langle \xi - |, & \bar{u}_+(\xi) &= [\xi| \equiv \langle \xi + |. \end{aligned} \quad (9)$$

Although we don't really need these notations for  $e^+e^- \rightarrow \mu^+\mu^-\gamma$ , they are now standard. Therefore, it is important for students to get to know them by reading modern review literature [25, 26, 27].

For massless spinors the following identities proved to be useful [19]. The reversion identity:

$$\bar{u}_{\lambda_1}(p_1) \Gamma u_{\lambda_2}(p_2) = \lambda_1 \lambda_2 \bar{u}_{-\lambda_2}(p_2) \Gamma^R u_{-\lambda_1}(p_1), \quad (10)$$

where  $\Gamma$  stands for any string of Dirac matrices and  $\Gamma^R$  is the same string written in reversed order.

The Chisholm identity:

$$\{\bar{u}_\lambda(p_1) \gamma^\mu u_\lambda(p_2)\} \gamma_\mu = 2u_\lambda(p_2) \bar{u}_\lambda(p_1) + 2u_{-\lambda}(p_1) \bar{u}_{-\lambda}(p_2). \quad (11)$$

These identities allow to get expression for any amplitude in terms of spinor inner products. For massless spinors the basic inner products are

$$\begin{aligned} [p_1 p_2] &= s(p_1, p_2) = \bar{u}_+(p_1) u_-(p_2) = -s(p_2, p_1), \\ \langle p_1 p_2 \rangle &= t(p_1, p_2) = \bar{u}_-(p_1) u_+(p_2) = [s(p_2, p_1)]^*. \end{aligned} \quad (12)$$

It is not difficult to get explicit expression for  $X = \sqrt{4p_1 \cdot \xi \, p_2 \cdot \xi} \, s(p_1, p_2)$ :

$$X = \bar{u}_-(\xi) \hat{p}_1 \hat{p}_2 u_+(\xi) = \bar{u}_-(\xi) \hat{p}_1 \hat{p}_2 \hat{\eta} u_-(\xi) = Sp \left\{ \omega_- \hat{\xi} \hat{p}_1 \hat{p}_2 \hat{\eta} \right\}.$$

Therefore

$$s(p_1, p_2) = \frac{p_1 \cdot \xi \, p_2 \cdot \eta - p_1 \cdot \eta \, p_2 \cdot \xi - i \epsilon_{\mu\nu\sigma\tau} \xi^\mu \eta^\nu p_1^\sigma p_2^\tau}{\sqrt{p_1 \cdot \xi \, p_2 \cdot \xi}}, \quad \epsilon_{0123} = 1.$$

Below we shall make Kleiss-Stirling [19] choice for the auxiliary vectors  $\xi$  and  $\eta$ :

$$\xi = (1, 1, 0, 0), \quad \eta = (0, 0, 1, 0). \quad (13)$$

Then

$$s(p_1, p_2) = (p_{1y} + ip_{1z}) \sqrt{\frac{p_{20} - p_{2x}}{p_{10} - p_{1x}}} - (p_{2y} + ip_{2z}) \sqrt{\frac{p_{10} - p_{1x}}{p_{20} - p_{2x}}}. \quad (14)$$

This formula is valid for any lightlike momenta  $p_1, p_2$  not collinear to  $\xi$ . The same is true for other formulas given above also. The case when one of the four-momenta is collinear to  $\xi$  have to be treated separately. In particular, we have

$$s(p, \xi) = s(\xi, p) = \sqrt{2p \cdot \xi},$$

for any lightlike four-momentum  $p$ .

Decomposition (8) allows to evaluate inner products

$$s_{\lambda_1, \lambda_2}(p_1, p_2) = \bar{u}_{\lambda_1}(p_1) u_{\lambda_2}(p_2)$$

for massive spinors. In particular  $s_{+-}(p_1, p_2) = -s_{+-}(p_2, p_1)$  is given by the very formula (14) and  $s_{-+}(p_1, p_2) = -[s_{+-}(p_1, p_2)]^*$ . While the equal helicity inner products depend explicitly on the masses (of course, for massive particles helicity is not a Lorentz-invariant concept. nevertheless we shall use this terminology in massive case too as some useful convention):

$$s_{++}(p_1, p_2) = s_{++}(p_2, p_1) = s_{--}(p_1, p_2) = m_1 \sqrt{\frac{p_2 \cdot \xi}{p_1 \cdot \xi}} + m_2 \sqrt{\frac{p_1 \cdot \xi}{p_2 \cdot \xi}} = m_1 \sqrt{\frac{p_{20} - p_{2x}}{p_{10} - p_{1x}}} + m_2 \sqrt{\frac{p_{10} - p_{1x}}{p_{20} - p_{2x}}}. \quad (15)$$

Inner products for antiparticle spinors are obtained by the following simple rule (as (8) indicates): substitute  $m \rightarrow -m$ ,  $\lambda \rightarrow -\lambda$  into the rhs of (14) and (15) when in the lhs  $u_\lambda(p)$ ,  $p^2 = m^2$  spinor is replaced by  $v_\lambda(p)$  antiparticle spinor.

It turns out [30] that the most numerically stable way of computing the scalar product  $p_1 \cdot p_2$ , especially when the masses are zero or small, is to use the formula

$$p_1 \cdot p_2 = \frac{1}{4} \sum_{\lambda_1, \lambda_2} |s_{\lambda_1, \lambda_2}(p_1, p_2)|^2 - m_1 m_2, \quad (16)$$

which can be proved by using the explicit forms for  $s_{\lambda_1, \lambda_2}(p_1, p_2)$  as given by (14) and (15).

To end our discussion of spinors, let us mention another interesting identity (the Schouten identity):

$$s_{+-}(p_1, p_2) s_{+-}(p_3, p_4) + s_{+-}(p_2, p_3) s_{+-}(p_1, p_4) + s_{+-}(p_3, p_1) s_{+-}(p_2, p_4) = 0. \quad (17)$$

The most easy way to check it is to use (14) and some computer program for algebraic manipulations, for example REDUCE [31].

## 2.4 Photon polarization four-vectors

The next important ingredient of the spinor technique under discussion is a convenient choice of the photon polarization four-vector. This polarization four-vector  $\epsilon_\lambda^\mu$  corresponding to a state of definite helicity  $\lambda = \pm 1$  should satisfy the equations

$$\epsilon_\lambda \cdot k = 0, \quad \epsilon_\lambda \cdot \epsilon_\lambda = 0, \quad \epsilon_\lambda^* \cdot \epsilon_\lambda = -1, \quad (18)$$

$k$  being the photon momentum. The following choice proved to be useful:

$$(\epsilon_\lambda^\mu(k; p))^* = \frac{\bar{u}_\lambda(k) \gamma^\mu u_\lambda(p)}{\sqrt{2} s_{-\lambda, \lambda}(k, p)}. \quad (19)$$

Here  $p$  is some auxiliary lightlike four-vector not collinear to  $k$  or  $\xi$ . It can be checked that (19) indeed satisfies relations (18). For example, using

$$|s_{-\lambda,\lambda}(k,p)|^2 = 2k \cdot p$$

and

$$\bar{u}_\lambda(k)\gamma^\mu u_\lambda(p)\bar{u}_\lambda(p)\gamma_\mu u_\lambda(k) = Sp \left\{ \omega_\lambda \hat{k} \gamma^\mu \omega_\lambda \hat{p} \gamma_\mu \right\} = Sp \left\{ \omega_\lambda \hat{k} \gamma^\mu \hat{p} \gamma_\mu \right\} = -4k \cdot p$$

we get  $\epsilon_\lambda^*(k;p) \cdot \epsilon_\lambda(k;p) = -1$ . Following [15], we keep in (19) explicit complex conjugation which for outgoing photons is canceled by another conjugation required by the Feynman rules.

Any other four-vector satisfying (18) is as good as (19) itself to represent the photon polarization and therefore can differ from (19) only by a phase and some gauge transformation. In particular, for another choice of the auxiliary four-vector we will have

$$\epsilon_\lambda^\mu(k;q) = e^{i\Phi(q,p)} \epsilon_\lambda^\mu(k;p) + \beta_\lambda(q,p,k) k_\mu.$$

Let us calculate the phase  $\Phi(q,p)$ .

$$e^{i\Phi(q,p)} = -\epsilon_\lambda^*(k,p) \cdot \epsilon_\lambda(k,q) = -\frac{\bar{u}_\lambda(k)\gamma^\mu u_\lambda(p)\bar{u}_\lambda(q)\gamma_\mu u_\lambda(k)}{2s_{-\lambda,\lambda}(k,p)s_{-\lambda,\lambda}^*(k,q)}.$$

Using the Chisholm identity (11) the numerator can be rewritten as follows

$$\bar{u}_\lambda(k) \{ \bar{u}_\lambda(q)\gamma_\mu u_\lambda(k) \} \gamma^\mu u_\lambda(p) =$$

$$2\bar{u}_\lambda(k) [u_{-\lambda}(q)\bar{u}_{-\lambda}(k) + u_\lambda(k)\bar{u}_\lambda(q)] u_\lambda(p) = 2s_{\lambda,-\lambda}(k,q)s_{-\lambda,\lambda}(k,p).$$

But  $s_{\lambda,-\lambda}(k,q) = -s_{-\lambda,\lambda}^*(k,q)$  and we get

$$e^{i\Phi(q,p)} = 1.$$

So

$$\epsilon_\lambda^\mu(k;q) = \epsilon_\lambda^\mu(k;p) + \beta_\lambda(q,p,k) k_\mu \quad (20)$$

and for each gauge invariant subset of diagrams we can choose the auxiliary four-vector  $p$  completely arbitrarily without generating relative complex phases – certainly a nice property.

Using the Chisholm identity again we get

$$\hat{\epsilon}_\lambda^*(k;p) = \frac{\sqrt{2}}{s_{-\lambda,\lambda}(k,p)} [u_\lambda(p)\bar{u}_\lambda(k) + u_{-\lambda}(k)\bar{u}_{-\lambda}(p)]. \quad (21)$$

From this relation the following “magic” identities follow

$$\hat{\epsilon}_\lambda^*(k;p)u_\lambda(p) = \hat{\epsilon}_\lambda^*(k;p)v_{-\lambda}(p) = \bar{v}_\lambda(p)\hat{\epsilon}_\lambda^*(k;p) = \bar{u}_{-\lambda}(p)\hat{\epsilon}_\lambda^*(k;p) = 0. \quad (22)$$

In fact our polarization four-vector (19) corresponds to the axial gauge  $p \cdot \epsilon_\lambda = 0$  and for the photon polarization sum we have

$$\sum_\lambda \epsilon_\lambda^\mu(k;p) \epsilon_\lambda^{*\nu}(k;p) = -g^{\mu\nu} + \frac{p^\mu k^\nu + p^\nu k^\mu}{p \cdot k}. \quad (23)$$

Indeed

$$\sum_\lambda \epsilon_\lambda^\mu \epsilon_\lambda^{*\nu} = \frac{\sum_\lambda \bar{u}_\lambda(p)\gamma^\mu u_\lambda(k)\bar{u}_\lambda(k)\gamma^\nu u_\lambda(p)}{4k \cdot p} = \frac{\sum_\lambda Sp \left\{ \omega_\lambda \hat{p} \gamma^\mu \omega_\lambda \hat{k} \gamma^\nu \right\}}{4k \cdot p} =$$

$$\frac{Sp \left\{ \sum_{\lambda} \omega_{\lambda} \hat{p} \gamma^{\mu} \hat{k} \gamma^{\nu} \right\}}{4k \cdot p} = \frac{Sp \left\{ \hat{p} \gamma^{\mu} \hat{k} \gamma^{\nu} \right\}}{4k \cdot p} = -g^{\mu\nu} + \frac{k^{\mu} p^{\nu} + k^{\nu} p^{\mu}}{p \cdot k}.$$

Substituting  $\hat{p} = u_{\lambda}(p) \bar{u}_{\lambda}(p) + u_{-\lambda}(p) \bar{u}_{-\lambda}(p)$  in

$$p \cdot \epsilon_{\lambda}^*(k; q) = \frac{\bar{u}_{\lambda}(k) \hat{p} u_{\lambda}(q)}{\sqrt{2} s_{-\lambda, \lambda}(k, q)}$$

we get

$$p \cdot \epsilon_{\lambda}^*(k; q) = \frac{s_{\lambda, -\lambda}(k, p) s_{-\lambda, \lambda}(p, q)}{\sqrt{2} s_{-\lambda, \lambda}(k, q)}. \quad (24)$$

In particular

$$p \cdot \epsilon_{\lambda}^*(k; p) = k \cdot \epsilon_{\lambda}^*(k; p) = 0. \quad (25)$$

The relation (24) allows to calculate  $\beta_{\lambda}(q, p, k)$  in (20):

$$\beta_{\lambda}(q, p, k) = \frac{\sqrt{2} s_{-\lambda, \lambda}(p, q)}{s_{-\lambda, \lambda}(p, k) s_{-\lambda, \lambda}(k, q)}. \quad (26)$$

## 2.5 $Z$ -functions as building blocks for helicity amplitudes

The following  $Z$ -functions are useful [32, 33] building blocks for helicity amplitudes:

$$Z_{\lambda_1, \lambda_2, \lambda_3, \lambda_4}^{\epsilon_1, \epsilon_2, \epsilon_3, \epsilon_4}(p_1, p_2, p_3, p_4) = \bar{u}_{\lambda_1}(p_1) \gamma_{\mu} u_{\lambda_2}(p_2) \bar{u}_{\lambda_3}(p_3) \gamma^{\mu} u_{\lambda_4}(p_4), \quad (27)$$

where it is assumed that every mass in this expression is written in the form  $\epsilon_i m_i$ , with  $\epsilon_i = 0, \pm 1$ , to ensure a simple use of the  $\lambda \rightarrow -\lambda$ ,  $m \rightarrow -m$  substitution rule for antiparticle spinors. Decomposition (8) of massive spinors in terms of massless ones allows to express  $Z$ -functions through spinor inner products. The calculation is straightforward although rather lengthy. To present the results let us introduce for a moment a shorthand notations

$$Z(\lambda_1, \lambda_2, \lambda_3, \lambda_4) \equiv Z_{\lambda_1, \lambda_2, \lambda_3, \lambda_4}^{\epsilon_1, \epsilon_2, \epsilon_3, \epsilon_4}(p_1, p_2, p_3, p_4), \quad \chi_i = \sqrt{2 p_i \cdot \xi}, \quad \mu_i = \frac{\epsilon_i m_i}{\chi_i}.$$

Then for half of the possible helicity configurations we have

$$\begin{aligned} Z(+, +, +, +) &= -2 [s_{+-}(p_1, p_3) s_{-+}(p_2, p_4) - \mu_1 \mu_2 \chi_3 \chi_4 - \mu_3 \mu_4 \chi_1 \chi_2], \\ Z(+, +, +, -) &= 2 \chi_2 [\mu_3 s_{+-}(p_1, p_4) - \mu_4 s_{+-}(p_1, p_3)], \\ Z(+, +, -, +) &= 2 \chi_1 [\mu_3 s_{-+}(p_2, p_4) - \mu_4 s_{-+}(p_2, p_3)], \\ Z(+, +, -, -) &= -2 [s_{+-}(p_1, p_4) s_{-+}(p_2, p_3) - \mu_1 \mu_2 \chi_3 \chi_4 - \mu_3 \mu_4 \chi_1 \chi_2], \\ Z(+, -, +, +) &= 2 \chi_4 [\mu_2 s_{+-}(p_1, p_3) - \mu_1 s_{+-}(p_2, p_3)], \\ Z(+, -, +, -) &= 0, \\ Z(+, -, -, +) &= 2 [\mu_1 \mu_3 \chi_2 \chi_4 + \mu_2 \mu_4 \chi_1 \chi_3 - \mu_1 \mu_4 \chi_2 \chi_3 - \mu_2 \mu_3 \chi_1 \chi_4], \\ Z(+, -, -, -) &= 2 \chi_3 [\mu_2 s_{+-}(p_1, p_4) - \mu_1 s_{+-}(p_2, p_4)]. \end{aligned} \quad (28)$$

The remaining half can be obtained by exchanging  $+$   $\leftrightarrow$   $-$  in the above expressions.

For illustration purposes let us sketch the derivation of  $Z(+, +, +, +)$ . Using the decomposition (8) we get (note that  $\bar{u}_{\pm}(p) \gamma_{\mu} u_{\mp}(q) = 0$  for lightlike four-momenta  $p$  and  $q$  because for such momenta  $u_{\pm}$  are chirality eigenstates)

$$Z(+, +, +, +) = [\bar{u}_{+}(p_1 \xi) \gamma_{\mu} u_{+}(p_2 \xi) + \mu_1 \mu_2 \bar{u}_{-}(\xi) \gamma_{\mu} u_{-}(\xi)] \times$$

$$[\bar{u}_+(p_{3\xi})\gamma^\mu u_+(p_{4\xi}) + \mu_3\mu_4\bar{u}_-(\xi)\gamma^\mu u_-(\xi)].$$

For lightlike four-momenta (but not for  $\xi$  which plays a special role in our construction [15]) we can enjoy the Chisholm identity (11) and obtain

$$\begin{aligned} \bar{u}_+(p_{1\xi})\gamma_\mu u_+(p_{2\xi})\bar{u}_+(p_{3\xi})\gamma^\mu u_+(p_{4\xi}) = \\ 2\bar{u}_+(p_{3\xi})[u_+(p_{2\xi})\bar{u}_+(p_{1\xi}) + u_-(p_{1\xi})\bar{u}_-(p_{2\xi})]u_+(p_{4\xi}) = \\ 2s_{+-}(p_{3\xi}, p_{1\xi})s_{+-}(p_{2\xi}, p_{4\xi}) = -2s_{+-}(p_1, p_3)s_{+-}(p_2, p_4). \end{aligned}$$

The last step follows from  $s_{\pm\mp}(p_\xi, q_\xi) = s_{\pm\mp}(p, q) = -s_{\pm\mp}(q, p)$ . Analogously

$$\begin{aligned} \bar{u}_+(p_{1\xi})\gamma_\mu u_+(p_{2\xi})\bar{u}_-(\xi)\gamma^\mu u_-(\xi) = \\ 2\bar{u}_-(\xi)[u_+(p_{2\xi})\bar{u}_+(p_{1\xi}) + u_-(p_{1\xi})\bar{u}_-(p_{2\xi})]u_-(\xi) = \\ 2s_{-+}(\xi, p_{2\xi})s_{-+}(p_{1\xi}, \xi) = 2\chi_2\chi_1. \end{aligned}$$

At last, because  $\xi^2 = 0$ , we have

$$\begin{aligned} \bar{u}_-(\xi)\gamma_\mu u_-(\xi)\bar{u}_-(\xi)\gamma^\mu u_-(\xi) = \\ Sp\left\{\omega_-\hat{\xi}\gamma_\mu\omega_-\hat{\xi}\gamma^\mu\right\} = Sp\left\{\omega_-\hat{\xi}\gamma_\mu\hat{\xi}\gamma^\mu\right\} = -2Sp\left\{\omega_-\hat{\xi}\hat{\xi}\right\} = 0. \end{aligned}$$

Putting all pieces together, hence the first line of (28) follows.

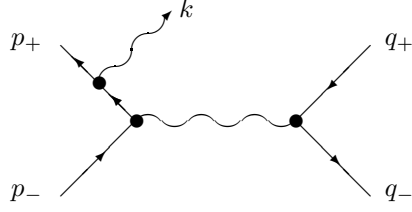
### 3 Tree level helicity amplitudes

Feynman diagrams for the process  $e^-(p_-) + e^+(p_+) \rightarrow \mu^-(q_-) + \mu^+(q_+) + \gamma(k)$  at tree level are naturally divided into two gauge-invariant subsets: initial state radiation and final state radiation.

#### 3.1 Initial state radiation

Let us consider the initial state radiation first. The helicity amplitude method gives especially simple and elegant results in massless case. For our radiative return studies we can neglect the electron mass assuming that the tagged hard photon is not emitted at very small angles. But unfortunately we can not neglect the muon mass if we are interested in production of the muon-antimuon pairs with sufficiently small invariant masses. For massless fermions helicity is not changed by photon emission. That is the helicity is conserved along initial electron line. Therefore the helicity amplitude  $\mathcal{A}_{\lambda_-^e, -\lambda_+^e, \lambda_-^\mu, -\lambda_+^\mu, \lambda_\gamma}$  is zero if  $\lambda_-^e = \lambda_+^e$  (note that the incoming positron with helicity  $\lambda_+^e$  is equivalent to the outgoing electron with helicity  $-\lambda_+^e$ ). So in our approximation of massless electron we have to consider only helicity amplitudes with opposite electron and positron helicities.

Let us consider in some details the calculation of  $\mathcal{A}_{+,+, \lambda_3, \lambda_4, +}^{(ISR)}$ . Because of the “magic” identities (22), in this case it is convenient to choose the auxiliary vector  $p$  in the photon polarization four-vector definition (19) to be the electron momentum  $p_-$ . Then only one initial state radiation diagram will contribute. Namely the one with the photon radiation from the positron:



According to the Feynman rules it is straightforward to get

$$\mathcal{A} = \frac{ie^3}{s'} \frac{1}{-2p_+ \cdot k} \bar{v}_-(p_+) \hat{\epsilon}_+^*(k; p_-) (-\hat{p}_+ + \hat{k}) \gamma_\mu u_+(p_-) \bar{u}_{\lambda_3}(q_-) \gamma^\mu v_{-\lambda_4}(q_+),$$

where  $s' = (q_- + q_+)^2$ . Because  $\bar{v}_-(p_+) \hat{\epsilon}_+^*(k; p_-) \hat{p}_+ = 2p_+ \cdot \epsilon_+^*(k; p_-) \bar{v}_-(p_+)$ , we will have  $\mathcal{A} = \mathcal{A}_1 + \mathcal{A}_2$ , where

$$\mathcal{A}_1 = \frac{ie^3}{s'} \frac{p_+ \cdot \epsilon_+^*(k; p_-)}{p_+ \cdot k} \bar{v}_-(p_+) \gamma_\mu u_+(p_-) \bar{u}_{\lambda_3}(q_-) \gamma^\mu v_{-\lambda_4}(q_+).$$

Using (24) and  $2p_+ \cdot k = -s_{+-}(k, p_+)s_{-+}(k, p_+)$ , we get

$$\mathcal{A}_1 = \frac{i\sqrt{2}e^3}{s'} \frac{s_{-+}(p_-, p_+)}{s_{-+}(k, p_-)s_{-+}(k, p_+)} Z_{+,+, \lambda_3, \lambda_4}^{0,0,1,-1}(p_+, p_-, q_-, q_+).$$

For  $\mathcal{A}_2$  we have

$$\mathcal{A}_2 = \frac{ie^3}{s'} \frac{1}{-2p_+ \cdot k} \bar{v}_-(p_+) \hat{\epsilon}_+^*(k; p_-) \hat{k} \gamma_\mu u_+(p_-) \bar{u}_{\lambda_3}(q_-) \gamma^\mu v_{-\lambda_4}(q_+).$$

Now  $\hat{\epsilon}_+^*(k; p_-) \hat{k} \gamma_\mu u_+(p_-) = -\hat{k} \hat{\epsilon}_+^*(k; p_-) \gamma_\mu u_+(p_-) = -2\epsilon_{+\mu}^*(k; p_-) \hat{k} u_+(p_-)$ , because  $k \cdot \epsilon_+^*(k; p_-) = 0$  and  $\hat{\epsilon}_+^*(k; p_-) u_+(p_-) = 0$ . Therefore

$$\mathcal{A}_2 = \frac{ie^3}{s'} \frac{1}{p_+ \cdot k} \bar{v}_-(p_+) \hat{k} u_+(p_-) \bar{u}_{\lambda_3}(q_-) \hat{\epsilon}_+^*(k; p_-) v_{-\lambda_4}(q_+).$$

The first spinor factor is calculated by substituting  $\bar{v}_-(p_+) = \bar{u}_+(p_+)$  and  $\hat{k} = u_+(k) \bar{u}_+(k) + u_-(k) \bar{u}_-(k)$ . The result is

$$\bar{v}_-(p_+) \hat{k} u_+(p_-) = s_{+-}(p_+, k) s_{-+}(k, p_-).$$

For the second spinor factor we have

$$\begin{aligned} \bar{u}_{\lambda_3}(q_-) \hat{\epsilon}_+^*(k; p_-) v_{-\lambda_4}(q_+) &= \\ \frac{\bar{u}_+(k) \gamma_\mu u_+(p_-) \bar{u}_{\lambda_3}(q_-) \gamma^\mu v_{-\lambda_4}(q_+)}{\sqrt{2}s_{-+}(k, p_-)} &= \frac{Z_{+,+, \lambda_3, \lambda_4}^{0,0,1,-1}(k, p_-, q_-, q_+)}{\sqrt{2}s_{-+}(k, p_-)}. \end{aligned}$$

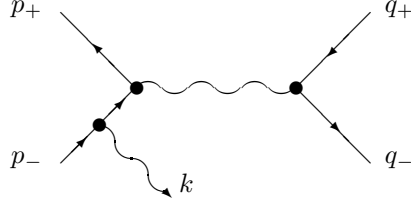
Combining all pieces together, we get

$$\mathcal{A}_2 = -\frac{i\sqrt{2}e^3}{s'} \frac{s_{-+}(p_-, k)}{s_{-+}(k, p_-)s_{-+}(k, p_+)} Z_{+,+, \lambda_3, \lambda_4}^{0,0,1,-1}(k, p_-, q_-, q_+)$$

and

$$\begin{aligned} \mathcal{A}_{+,+, \lambda_3, \lambda_4, +}^{(ISR)} &= \frac{i\sqrt{2}e^3}{s'} \times \\ \frac{s_{-+}(p_-, p_+) Z_{+,+, \lambda_3, \lambda_4}^{0,0,1,-1}(p_+, p_-, q_-, q_+) - s_{-+}(p_-, k) Z_{+,+, \lambda_3, \lambda_4}^{0,0,1,-1}(k, p_-, q_-, q_+)}{s_{-+}(k, p_-)s_{-+}(k, p_+)} &. \end{aligned} \quad (29)$$

For  $\mathcal{A}_{+,+, \lambda_3, \lambda_4, -}^{(ISR)}$  it is useful to take  $p = p_+$  as the auxiliary four-vector for the photon polarization. Then only the following diagram will contribute:



We can proceed as above and obtain

$$\mathcal{A}_{+,+, \lambda_3, \lambda_4, -}^{(ISR)} = \frac{i\sqrt{2}e^3}{s'} \times \frac{s_{+-}(p_-, p_+)Z_{+,+, \lambda_3, \lambda_4}^{0,0,1,-1}(p_+, p_-, q_-, q_+) - s_{+-}(k, p_+)Z_{+,+, \lambda_3, \lambda_4}^{0,0,1,-1}(p_+, k, q_-, q_+)}{s_{+-}(k, p_-)s_{+-}(k, p_+)}. \quad (30)$$

We do not give any calculation details because they completely resemble the ones described for  $\mathcal{A}_{+,+, \lambda_3, \lambda_4, +}^{(ISR)}$ . Maybe only just one little difference deserves to be commented: in calculation of

$$\bar{u}_{\lambda_3}(q_-)\hat{\epsilon}_-^*(k; p_+)v_{-\lambda_4}(q_+) = \frac{\bar{u}_-(k)\gamma^\mu u_-(p_+)\bar{u}_{\lambda_3}(q_-)\gamma_\mu v_{-\lambda_4}(q_+)}{\sqrt{2}s_{+-}(k, p_+)}$$

one needs to use the line-reversal identity (10)

$$\bar{u}_-(k)\gamma^\mu u_-(p_+) = \bar{u}_+(p_+)\gamma^\mu u_+(k)$$

to obtain

$$\bar{u}_{\lambda_3}(q_-)\hat{\epsilon}_-^*(k; p_+)v_{-\lambda_4}(q_+) = \frac{Z_{+,+, \lambda_3, \lambda_4}^{0,0,1,-1}(p_+, k, q_-, q_+)}{\sqrt{2}s_{+-}(k, p_+)}.$$

The remaining helicity amplitudes for initial state radiation are calculated analogously (or they can be obtained by the parity invariance argument for free). The results are

$$\mathcal{A}_{-,-, \lambda_3, \lambda_4, +}^{(ISR)} = \frac{i\sqrt{2}e^3}{s'} \times \frac{s_{-+}(p_-, p_+)Z_{-,-, \lambda_3, \lambda_4}^{0,0,1,-1}(p_+, p_-, q_-, q_+) - s_{-+}(k, p_+)Z_{-,-, \lambda_3, \lambda_4}^{0,0,1,-1}(p_+, k, q_-, q_+)}{s_{-+}(k, p_-)s_{-+}(k, p_+)}. \quad (31)$$

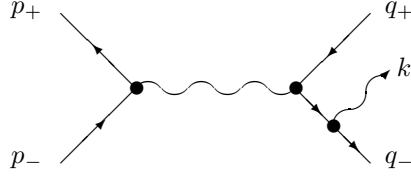
and

$$\mathcal{A}_{-,-, \lambda_3, \lambda_4, -}^{(ISR)} = \frac{i\sqrt{2}e^3}{s'} \times \frac{s_{+-}(p_-, p_+)Z_{-,-, \lambda_3, \lambda_4}^{0,0,1,-1}(p_+, p_-, q_-, q_+) - s_{+-}(p_-, k)Z_{-,-, \lambda_3, \lambda_4}^{0,0,1,-1}(k, p_-, q_-, q_+)}{s_{+-}(k, p_-)s_{+-}(k, p_+)}. \quad (32)$$

### 3.2 Final state radiation

For the final state radiation both possible diagrams contribute owing to the nonzero muon mass. So we will not try to get any compact expressions for  $\mathcal{A}^{(FSR)}$ , even of the kind we had for  $\mathcal{A}^{(ISR)}$ . Instead we will follow the philosophy of [32] and will express the corresponding amplitudes in terms of the  $Z$ -functions assuming further numerical evaluation on a computer.

Let us consider the photon emission from the outgoing muon:



The corresponding contribution to the  $\mathcal{A}_{\lambda_1, \lambda_1, \lambda_3, \lambda_4, \lambda}^{(FSR)}$  helicity amplitude has the form

$$\mathcal{A} = \frac{ie^3}{s} \frac{1}{2q_- \cdot k} \bar{v}_{-\lambda_1}(p_+) \gamma_\mu u_{\lambda_1}(p_-) \bar{u}_{\lambda_3}(q_-) \hat{\epsilon}_\lambda^*(k; p) (\hat{q}_- + m_\mu + \hat{k}) \gamma^\mu v_{-\lambda_4}(q_+),$$

where  $s = (p_- + p_+)^2$ . Using

$$\hat{\epsilon}_\lambda^*(k; p) = \frac{\bar{u}_\lambda(k) \gamma^\mu u_\lambda(p)}{\sqrt{2} s_{-\lambda, \lambda}(k, p)} \gamma_\mu$$

and decomposing again  $\mathcal{A} = \mathcal{A}_1 + \mathcal{A}_2$ , where  $\mathcal{A}_1$  corresponds to the part originated from

$$\hat{q}_- + m_\mu = u_+(q_-) \bar{u}_+(q_-) + u_-(q_-) \bar{u}_-(q_-)$$

and  $\mathcal{A}_2$  – to the part originated from

$$\hat{k} = u_+(k) \bar{u}_+(k) + u_-(k) \bar{u}_-(k),$$

we get

$$\mathcal{A}_1 = \frac{ie^3}{s} \frac{1}{2q_- \cdot k} \frac{X_+^{(1)} + X_-^{(1)}}{\sqrt{2} s_{-\lambda, \lambda}(k, p)}.$$

Here

$$X_+^{(1)} = \bar{v}_{-\lambda_1}(p_+) \gamma_\mu u_{\lambda_1}(p_-) \bar{u}_{\lambda_3}(q_-) \bar{u}_\lambda(k) \gamma^\nu u_\lambda(p) \gamma_\nu u_+(q_-) \bar{u}_+(q_-) \gamma^\mu v_{-\lambda_4}(q_+) = \\ \bar{v}_{-\lambda_1}(p_+) \gamma_\mu u_{\lambda_1}(p_-) \bar{u}_+(q_-) \gamma^\mu v_{-\lambda_4}(q_+) \bar{u}_\lambda(k) \gamma^\nu u_\lambda(p) \bar{u}_{\lambda_3}(q_-) \gamma_\nu u_+(q_-).$$

Therefore

$$X_+^{(1)} = Z_{\lambda_1, \lambda_1, +, \lambda_4}^{0, 0, 1, -1}(p_+, p_-, q_-, q_+) * Z_{\lambda, \lambda, \lambda_3, +}^{0, 0, 1, 1}(k, p, q_-, q_-). \quad (33)$$

$X_-^{(1)}$  is obtained from  $X_+^{(1)}$  simply by reversing the intermediate helicity sign:

$$X_-^{(1)} = Z_{\lambda_1, \lambda_1, -, \lambda_4}^{0, 0, 1, -1}(p_+, p_-, q_-, q_+) * Z_{\lambda, \lambda, \lambda_3, -}^{0, 0, 1, 1}(k, p, q_-, q_-). \quad (34)$$

$\mathcal{A}_2$  is dealt with an analogous way as well as contributions from the diagram with the photon emission from the outgoing  $\mu^+$ . So we skip the details and give the final result

$$\mathcal{A}_{\lambda_1, \lambda_1, \lambda_3, \lambda_4, \lambda}^{(FSR)} = \frac{ie^3}{s} \frac{1}{2\sqrt{2} s_{-\lambda, \lambda}(k, p)} \times \left\{ \frac{X_+^{(1)} + X_-^{(1)} + X_+^{(2)} + X_-^{(2)}}{k \cdot q_-} - \frac{X_+^{(3)} + X_-^{(3)} + X_+^{(4)} + X_-^{(4)}}{k \cdot q_+} \right\}. \quad (35)$$

$X_{\pm}^{(1)}$  were defined above by (33) and (34). For the remaining  $X_{\pm}^{(i)}$  functions the corresponding expressions are given below:

$$\begin{aligned} X_+^{(2)} &= Z_{\lambda_1, \lambda_1, +, \lambda_4}^{0, 0, 0, -1}(p_+, p_-, k, q_+) * Z_{\lambda, \lambda, \lambda_3, +}^{0, 0, 1, 0}(k, p, q_-, k), \\ X_-^{(2)} &= Z_{\lambda_1, \lambda_1, -, \lambda_4}^{0, 0, 0, -1}(p_+, p_-, k, q_+) * Z_{\lambda, \lambda, \lambda_3, -}^{0, 0, 1, 0}(k, p, q_-, k), \\ X_+^{(3)} &= Z_{\lambda_1, \lambda_1, \lambda_3, +}^{0, 0, 1, -1}(p_+, p_-, q_-, q_+) * Z_{\lambda, \lambda, +, \lambda_4}^{0, 0, -1, -1}(k, p, q_+, q_+), \\ X_-^{(3)} &= Z_{\lambda_1, \lambda_1, \lambda_3, -}^{0, 0, 1, -1}(p_+, p_-, q_-, q_+) * Z_{\lambda, \lambda, -, \lambda_4}^{0, 0, -1, -1}(k, p, q_+, q_+), \\ X_+^{(4)} &= Z_{\lambda_1, \lambda_1, \lambda_3, +}^{0, 0, 1, 0}(p_+, p_-, q_-, k) * Z_{\lambda, \lambda, +, \lambda_4}^{0, 0, 0, -1}(k, p, k, q_+), \\ X_-^{(4)} &= Z_{\lambda_1, \lambda_1, \lambda_3, -}^{0, 0, 1, 0}(p_+, p_-, q_-, k) * Z_{\lambda, \lambda, -, \lambda_4}^{0, 0, 0, -1}(k, p, k, q_+). \end{aligned} \quad (36)$$

To facilitate the massless limit, we make the following helicity-dependent choice for the auxiliary four-vector  $p$ :

$$p = \begin{cases} q_+ \xi, & \text{if } \lambda \lambda_4 = +1, \\ q_- \xi, & \text{if } \lambda \lambda_4 = -1. \end{cases} \quad (37)$$

### 3.3 Squared matrix element in the massless limit

Let us check our helicity amplitudes against  $m_\mu \rightarrow 0$  massless limit. For illustration we will sketch the derivation of the limit for  $\mathcal{A}_{+, +, -, -, +}$ . In the massless limit we have  $s' = 2q_- \cdot q_+ = -s_{+-}(q_+, q_-)s_{-+}(q_+, q_-)$  and

$$Z(+, +, -, -) = -2s_{+-}(p_1, p_4)s_{-+}(p_2, p_3).$$

Therefore (29) takes the form

$$\mathcal{A}_{+, +, -, -, +}^{(ISR)} = 2\sqrt{2}ie^3 \times \frac{s_{-+}(p_-, q_-) [s_{-+}(p_-, p_+)s_{+-}(p_+, q_+) - s_{-+}(p_-, k)s_{+-}(k, q_+)]}{s_{+-}(q_+, q_-)s_{-+}(q_+, q_-)s_{-+}(k, p_-)s_{-+}(k, p_+)}.$$

But using four-momentum conservation  $p_- + p_+ = q_- + q_+ + k$  and the Dirac equation we get

$$\begin{aligned} [s_{-+}(p_-, p_+)s_{+-}(p_+, q_+) - s_{-+}(p_-, k)s_{+-}(k, q_+)] &= \\ \bar{u}_-(p_-) [u_+(p_+)\bar{u}_+(p_+) - u_+(k)\bar{u}_+(k)] u_-(q_+) &= \\ \bar{u}_-(p_-)\omega_+(\hat{p}_- - \hat{k})u_-(q_+) = \bar{u}_-(p_-)\omega_+(\hat{q}_- + \hat{q}_+ - \hat{p}_-)u_-(q_+) &= \\ \bar{u}_-(p_-)u_+(q_-)\bar{u}_+(q_-)u_-(q_+) = s_{-+}(p_-, q_-)s_{-+}(q_-, q_+), \end{aligned}$$

and  $\mathcal{A}_{+, +, -, -, +}^{(ISR)}$  is simplified to

$$\mathcal{A}_{+, +, -, -, +}^{(ISR)} = -2\sqrt{2}ie^3 \frac{s_{-+}^2(p_-, q_-)}{s_{-+}(q_+, q_-)s_{-+}(k, p_-)s_{-+}(k, p_+)} =$$

$$2ie^3 \frac{s_{-+}^2(p_-, q_-)}{s_{-+}(p_-, p_+)s_{-+}(q_-, q_+)} \beta_+(p_-, p_+, k), \quad (38)$$

Where  $\beta_+(p_+, p_-, k)$  is defined by (26). For the given helicity configuration, in the massless limit,  $p = q_-$  and all  $X_+^{(i)}$  functions in (35) equal zero.  $X_-^{(1)}$  and  $X_-^{(2)}$  are proportional to  $s_{-+}(q_-, q_-)$  and hence also are zeros. The only nonzero combinations are

$$X_-^{(3)} = 4s_{+-}(p_+, q_+)s_{-+}(p_-, q_-)s_{+-}(k, q_+)s_{-+}(q_-, q_+)$$

and

$$X_-^{(4)} = 4s_{+-}(p_+, k)s_{-+}(p_-, q_-)s_{+-}(k, q_+)s_{-+}(q_-, k).$$

So (35) is reduced to

$$\mathcal{A}_{+,+, -, -, +}^{(FSR)} = -2\sqrt{2}ie^3 \times \frac{s_{-+}(p_-, q_-)s_{+-}(k, q_+) [s_{+-}(p_+, q_+)s_{-+}(q_-, q_+) + s_{+-}(p_+, k)s_{-+}(q_-, k)]}{s \cdot 2k \cdot q_+ s_{-+}(k, q_-)}.$$

We can apply four-momentum conservation and the Dirac equation again to simplify

$$[s_{+-}(p_+, q_+)s_{-+}(q_-, q_+) + s_{+-}(p_+, k)s_{-+}(q_-, k)] = s_{+-}(p_-, p_+)s_{-+}(p_-, q_-).$$

Besides

$$s = 2p_- \cdot p_+ = -s_{+-}(p_-, p_+)s_{-+}(p_-, p_+), \quad 2k \cdot q_+ = -s_{+-}(k, q_+)s_{-+}(k, q_+).$$

Therefore

$$\begin{aligned} \mathcal{A}_{+,+, -, -, +}^{(FSR)} &= -2\sqrt{2}ie^3 \frac{s_{-+}^2(p_-, q_-)}{s_{-+}(p_-, p_+)s_{-+}(k, q_-)s_{-+}(k, q_+)} = \\ &- 2ie^3 \frac{s_{-+}^2(p_-, q_-)}{s_{-+}(p_-, p_+)s_{-+}(q_-, q_+)} \beta_+(q_-, q_+, k). \end{aligned} \quad (39)$$

Combining (38) and (39) we get in the massless limit

$$\mathcal{A}_{+,+, -, -, +} = 2ie^3 \frac{s_{-+}^2(p_-, q_-)}{s_{-+}(p_-, p_+)s_{-+}(q_-, q_+)} [\beta_+(p_-, p_+, k) - \beta_+(q_-, q_+, k)]. \quad (40)$$

This result agrees to the one given in [21] (note the sign difference in our definition of the photon polarization four-vector (19) compared to what is used in [21]).

The massless limit for other helicity configurations can be considered similarly and the results are given below:

$$\begin{aligned} \mathcal{A}_{+,+, -, -, -} &= 2ie^3 \frac{s_{-+}^2(p_+, q_+)}{s_{-+}(p_-, p_+)s_{-+}(q_-, q_+)} [\beta_-(p_-, p_+, k) - \beta_-(q_-, q_+, k)], \\ \mathcal{A}_{+,+, +, +, +} &= -2ie^3 \frac{s_{-+}^2(p_-, q_+)}{s_{-+}(p_-, p_+)s_{-+}(q_-, q_+)} [\beta_+(p_-, p_+, k) - \beta_+(q_-, q_+, k)], \\ \mathcal{A}_{+,+, +, +, -} &= -2ie^3 \frac{s_{-+}^2(p_+, q_-)}{s_{-+}(p_-, p_+)s_{-+}(q_-, q_+)} [\beta_-(p_-, p_+, k) - \beta_-(q_-, q_+, k)], \end{aligned} \quad (41)$$

The amplitudes for the remaining helicity configurations are obtained by simply reversing the signs of the helicity labels in the above given expressions (parity conjugation).

To evaluate the norms of the above given massless amplitudes, we will need  $|\beta_\lambda(p_-, p_+, k) - \beta_\lambda(q_-, q_+, k)|^2$ . Note that

$$\beta_\lambda(p_-, p_+, k) = \frac{p_+ \cdot \epsilon_\lambda(k, p_-)}{k \cdot p_+} = \frac{\bar{u}_\lambda(k) \hat{p}_+ u_\lambda(p_-)}{\sqrt{2k \cdot p_+ s_{-\lambda, \lambda}(k, p_-)}}. \quad (42)$$

Let us introduce a four-vector [34]<sup>2</sup>

$$v_p = \frac{p_+}{k \cdot p_+} - \frac{p_-}{k \cdot p_-}, \quad (43)$$

such that  $k \cdot v_p = 0$  and therefore  $\hat{k} \hat{v}_p = -\hat{v}_p \hat{k}$ . Then

$$\beta_\lambda(p_-, p_+, k) = \frac{\bar{u}_\lambda(k) \hat{v}_p u_\lambda(p_-)}{\sqrt{2s_{-\lambda, \lambda}(k, p_-)}}.$$

But

$$\bar{u}_\lambda(k) \hat{v}_p u_\lambda(p_-) = \frac{\bar{u}_{-\lambda}(\xi) \hat{k} \hat{v}_p u_\lambda(p_-)}{\sqrt{2k \cdot \xi}} = -\frac{\bar{u}_{-\lambda}(\xi) \hat{v}_p \hat{k} u_\lambda(p_-)}{\sqrt{2k \cdot \xi}}.$$

Substituting here  $\hat{k} = u_\lambda(k) \bar{u}_\lambda(k) + u_{-\lambda}(k) \bar{u}_{-\lambda}(k)$  we get

$$\bar{u}_\lambda(k) \hat{v}_p u_\lambda(p_-) = -s_{-\lambda, \lambda}(k, p_-) \frac{\bar{u}_{-\lambda}(\xi) \hat{v}_p u_{-\lambda}(k)}{\sqrt{2k \cdot \xi}}$$

and therefore

$$\beta_\lambda(p_-, p_+, k) = -\frac{\bar{u}_{-\lambda}(\xi) \hat{v}_p u_{-\lambda}(k)}{2\sqrt{k \cdot \xi}}. \quad (44)$$

Then it is easy to get

$$|\beta_\lambda(p_-, p_+, k)|^2 = \frac{Sp \left\{ \omega_{-\lambda} \hat{\xi} \hat{v}_p \hat{k} \hat{v}_p \right\}}{4k \cdot \xi}.$$

But  $\hat{v}_p \hat{k} \hat{v}_p = -v_p^2 \hat{k}$  and therefore we get

$$|\beta_\lambda(p_-, p_+, k)|^2 = -\frac{1}{2} v_p^2.$$

Analogously

$$\begin{aligned} \beta_\lambda(p_-, p_+, k) \beta_\lambda^*(q_-, q_+, k) + \beta_\lambda(q_-, q_+, k) \beta_\lambda^*(p_-, p_+, k) = \\ \frac{Sp \left\{ \omega_{-\lambda} \hat{\xi} \left( \hat{v}_p \hat{k} \hat{v}_q + \hat{v}_q \hat{k} \hat{v}_p \right) \right\}}{4k \cdot \xi} = -v_p \cdot v_q. \end{aligned}$$

Therefore

$$|\beta_\lambda(p_-, p_+, k) - \beta_\lambda(q_-, q_+, k)|^2 = -\frac{1}{2} (v_p - v_q)^2. \quad (45)$$

This equation enables to find the massless limit for the squared matrix element averaged over initial and summed over final polarizations as

$$\overline{|\mathcal{A}|^2} = -e^6 \frac{t^2 + u^2 + t'^2 + u'^2}{s s'} (v_p - v_q)^2, \quad (46)$$

<sup>2</sup> To motivate its introduction, note that the first term is already present in (42), and we can add any term proportional to  $p_-$  without changing the result, since  $\hat{p}_- u_\lambda(p_-) = 0$ . The proportionality coefficient is chosen so that  $\hat{k}$  and  $\hat{v}_p$  commute, as this will allow the calculation to be performed as described in the text.

where

$$\begin{aligned} s &= (p_- + p_+)^2, \quad t = -2p_+ \cdot q_+, \quad u = -2p_+ \cdot q_-, \\ s' &= (q_- + q_+)^2, \quad t' = -2p_- \cdot q_-, \quad u' = -2p_- \cdot q_+. \end{aligned} \quad (47)$$

This result also agrees to what is known in the literature [34,21] and can be used in the program as a testing tool for the tree level amplitude against bugs.

As an another testing tool we can use the hard bremsstrahlung squared amplitude from [35] which incorporates the nonzero muon mass. In our notations and for the massless electron this result is

$$|\overline{\mathcal{A}}|^2 = e^6 (R_{ini} + R_{fin} + R_{int}), \quad (48)$$

where individual contributions, from the initial state radiation, final state radiation and their interference, are given by

$$\begin{aligned} R_{ini} &= \frac{1}{s'x_1x_2} \left\{ t^2 + u^2 + t'^2 + u'^2 + 2m_\mu^2 \frac{(t+u)^2 + (t'+u')^2}{s'} \right\}, \\ R_{fin} &= \frac{1}{sy_1y_2} \left\{ \left[ t^2 + u'^2 + 2m_\mu^2 s \right] \left[ 1 - 2\frac{m_\mu^2}{s} \left( 1 + \frac{y_1}{y_2} \right) \right] + \right. \\ &\quad \left[ t'^2 + u^2 + 2m_\mu^2 s \right] \left[ 1 - 2\frac{m_\mu^2}{s} \left( 1 + \frac{y_2}{y_1} \right) \right] + 8\frac{m_\mu^2}{s} (x_1^2 + x_2^2) - 8m_\mu^2 (s - s') \right\}, \\ R_{int} &= \frac{1}{ss'x_1x_2y_1y_2} \left\{ \left( ux_2y_1 + u'x_1y_2 - tx_2y_2 - t'x_1y_1 \right) \times \right. \\ &\quad \left( t^2 + t'^2 + y^2 + u'^2 + 2m_\mu^2 (s + s') \right) + \\ &\quad \left. + 2m_\mu^2 x_1x_2 \left[ (s - s')(u + u' - t - t') - 4(x_1 - x_2)(y_1 - y_2) \right] \right\}, \end{aligned} \quad (49)$$

with

$$x_1 = k \cdot p_+, \quad x_2 = k \cdot p_-, \quad y_1 = k \cdot q_+, \quad y_2 = k \cdot q_-. \quad (50)$$

The same squared amplitude was calculated in [8]. Although the formulas look different, we have checked numerically in the massless electron limit that both [8] and [35] give the same result (after the  $\Delta_{s_1s_1}$  sign misprint had been corrected in formula (2.12) of [8]). Our helicity amplitudes presented above also have been checked numerically to lead to the same tree level  $e^-e^+ \rightarrow \mu^-\mu^+\gamma$  squared amplitude (48-49).

#### 4 Monte Carlo algorithm

The matrix element we have described in the previous section is strongly peaked in certain regions of the phase space. For this reason generating events distributed according to this matrix element efficiently is not a trivial task. In this section a detailed description of the Monte Carlo algorithm used in the event generator is given.

In the next subsection, we will start with some general remarks on how random numbers with a given probability distribution can be generated. In particular, we describe the acceptance-rejection algorithm that will be used in our Monte Carlo program. We then explain in separate subsections how the initial and final state radiations can be described by crude distributions that can be efficiently generated using combinations of analytic inversion and acceptance-rejection methods.

The separation into an initial-state crude distribution and the final-state crude distribution means that we are not considering the interference between them. This is done to facilitate the Monte Carlo generation of these distributions. The interference is automatically reintroduced in the last step of the acceptance-rejection algorithm because we use the ratio of the square of the actual amplitude to the sum of the squares of the initial-state and final-state crude amplitudes to calculate the acceptance-rejection weight.

For the acceptance-rejection method to be effective, it is important that the coarse distribution reproduces the main features of the real distribution. In our case, the physical origin of the various singularities of the distribution to be generated is that virtual fermions in the Feynman diagrams describing radiation from the initial and final states may appear near on-shell in some kinematic situations. For radiation in the initial state from a massless (in our approximation) electron or positron, this occurs for the collinear radiation or when a very soft photon is emitted. For radiation from a muon or anti-muon in the final state, the peaked region in the amplitude corresponds to the emission of soft photons.

#### 4.1 General remarks

The most efficient way to generate random numbers with a given probability density  $f(x)$  is as follows. If we define

$$r = \int_{x_{min}}^x f(y)dy \equiv F(x), \quad (51)$$

then the probability that in a given event  $x$ -variable lays in the interval  $[x, x + dx]$  is  $f(x)dx = dr$ . However, this is also the probability that the variable  $r$  lays in the interval  $[r, r + dr]$ , where  $r = F(x)$ . Therefore  $r$ -variable is distributed uniformly. This gives the following algorithm to generate  $f(x)$  distribution (which will be assumed to be normalized in the interval  $[x_{min}, x_{max}]$ , although this is not too relevant):

- generate a random number  $r$  uniformly distributed in the interval  $[0, 1]$ .
- find  $x$  such that  $r = F(x)$ .

This is the so called analytic inversion method [36]. It is assumed that (51) gives an analytic expression for  $F(x)$  which can be easily inverted, at least numerically. Unfortunately this is not always the case. In such situations acceptance-rejection method turns out to be helpful. Suppose  $f_0(x)$  is some crude distribution which: 1) shares major features of desired  $f(x)$  distribution and 2) can be generated by analytic inversion. Then the acceptance-rejection algorithm to generate  $f(x)$ -distribution goes as follows [36,37]:

- generate a random number  $x$  according to the crude distribution  $f_0(x)$ .
- calculate the weight  $w = f(x)/f_0(x)$ .
- generate a random number  $r$  uniformly distributed in the interval  $[0, C]$ , where  $C$  is some number larger than maximal weight  $w_{max}$  (not far from it, however, if a good efficiency is desired).
- if  $r \leq w$ , accept the event, otherwise repeat the whole procedure.

The probability that the first step will produce  $x$ -variable in the interval  $[x, x + dx]$  is  $p_1 = f_0(x)dx$ , while the probability of accepting this event is  $p_2 = w/C$ . Therefore, the combined probability is

$$p = p_1 p_2 = \frac{1}{C} f_0(x) w dx = \frac{1}{C} f(x) dx$$

and the accepted events are indeed distributed according to the density function  $f(x)$ .

In our case we want to generate the distribution

$$d\sigma = \frac{\alpha^3}{8\pi^2 s} R \delta(Q - q_- - q_+) \frac{d\vec{q}_-}{E_-} \frac{d\vec{q}_+}{E_+} \frac{d\vec{k}}{\omega}, \quad (52)$$

where  $E_{\pm}$ ,  $\omega$  stand for the  $\mu^{\pm}$  and photon energies,  $Q = p_- + p_+ - k$ ,

$$R = \frac{|\overline{\mathcal{A}}|^2}{e^6}, \quad (53)$$

and the matrix element  $|\overline{\mathcal{A}}|^2$  was discussed earlier. The crude distribution, that models peculiar features of  $R$  consists of two parts

$$d\sigma_0 = d\sigma_0^{(ISR)} + d\sigma_0^{(FSR)}, \quad (54)$$

where the first one deals with initial state radiation and the second one with the final state radiation. The decision which part of the crude distribution to generate in each event is based on relative magnitudes of the corresponding total cross sections  $\sigma_0^{(ISR)}$  and  $\sigma_0^{(FSR)}$ . After event is generated according to the crude distribution, the acceptance-rejection method is applied to restore the real distribution.

Given the total number of events  $N_{tot}$ , generated with the crude distribution, and the number of accepted events  $N_{acc}$ , the total cross section can be calculated as

$$\sigma(e^+e^- \rightarrow \mu^+\mu^-\gamma) = \frac{N_{acc}}{N_{tot}} \left( \sigma_0^{(ISR)} + \sigma_0^{(FSR)} \right) C, \quad (55)$$

where  $C$  is the majoring value for the weights, since the acceptance probability of an average event is given by

$$p = \frac{1}{C} \frac{\sigma(e^+e^- \rightarrow \mu^+\mu^-\gamma)}{\sigma_0^{(ISR)} + \sigma_0^{(FSR)}}, \quad (56)$$

and, on the other hand,  $p = N_{acc}/N_{tot}$  for sufficiently large  $N_{tot}$ . Since  $N_{acc}$  is distributed according to the binomial distribution, for an error estimate one can take

$$\Delta\sigma = \sqrt{\frac{p(1-p)}{N_{tot}}} \left( \sigma_0^{(ISR)} + \sigma_0^{(FSR)} \right) C. \quad (57)$$

Now we describe in some details how  $d\sigma_0^{(ISR)}$  and  $d\sigma_0^{(FSR)}$  distributions are generated. Our treatment was inspired by [38,39,40], but explicit realization of the algorithms is original.

#### 4.2 Crude distribution for the initial state radiation

To approximate initial state radiation part of  $e^-e^+ \rightarrow \mu^-\mu^+\gamma$  matrix element, we use

$$R_0^{(ISR)} = \frac{1}{s'x_1x_2\beta^*} \left\{ (t+u)^2 + (t'+u')^2 \right\}, \quad (58)$$

where

$$\beta^* = \sqrt{1 - \frac{4m_\mu^2}{s'}}$$

is the muon velocity in the dimuon rest frame and other invariants used in (58) were defined earlier in (47) and (50).

After some trial and error, the form (58) was motivated by the second term in the  $R_{ini}$  expression in (49). The factor  $1/\beta^*$  was added to eliminate it after integration over the muon and antimuon momenta (see (59)).

Let us explain how  $d\sigma_0^{(ISR)}$  distribution is generated. First of all we need the corresponding energy and angular spectra of the photon. To get those, we integrate the distribution

$$d\sigma_0^{(ISR)} = \frac{\alpha^3}{8\pi^2 s} R_0^{(ISR)} \delta(Q - q_- - q_+) \frac{d\vec{q}_-}{E_-} \frac{d\vec{q}_+}{E_+} \frac{d\vec{k}}{\omega}$$

over the muon and antimuon momenta. But since

$$(t + u)^2 + (t' + u')^2 = 4 [(p_- \cdot Q)^2 + (p_+ \cdot Q)^2],$$

the integrand does not depend on muon and antimuon momenta. Using

$$\int \delta(Q - q_- - q_+) \frac{d\vec{q}_-}{E_-} \frac{d\vec{q}_+}{E_+} = 2\pi\beta^*, \quad (59)$$

we obtain after integrating over those momenta

$$d\sigma_0^{(ISR)} = \frac{\alpha^3}{\pi} \frac{1}{ss'x_1x_2} [(p_+ \cdot Q)^2 + (p_- \cdot Q)^2] \frac{d\vec{k}}{\omega}.$$

Using

$$\begin{aligned} (p_+ \cdot Q)^2 + (p_- \cdot Q)^2 &= \frac{1}{2} \left\{ [(p_+ + p_-) \cdot Q]^2 + [(p_+ - p_-) \cdot Q]^2 \right\} = \\ &= \frac{1}{2} \left\{ [s - (x_1 + x_2)]^2 + (x_1 - x_2)^2 \right\} = \frac{1}{2} \left\{ s^2 - 2s(x_1 + x_2) + 2(x_1^2 + x_2^2) \right\} \end{aligned}$$

and substituting

$$x_1 + x_2 = \frac{s - s'}{2}, \quad x_1^2 + x_2^2 = \frac{(s - s')^2}{4} - 2x_1x_2,$$

we obtain

$$(p_+ \cdot Q)^2 + (p_- \cdot Q)^2 = 2 \left[ \frac{s^2 + s'^2}{8} - x_1x_2 \right].$$

Therefore

$$\begin{aligned} d\sigma_0^{(ISR)} &= \frac{2\alpha^3}{\pi} \frac{1}{ss'} \left[ \frac{s^2 + s'^2}{8x_1x_2} - 1 \right] \frac{d\vec{k}}{\omega} = \\ &= \frac{4\alpha^3}{ss'} \left[ \frac{s^2 + s'^2}{2s\omega^2(1 - \cos^2 \theta)} - 1 \right] \omega d\omega d\cos \theta, \end{aligned} \quad (60)$$

where  $\theta$  stands for the photon polar angle.

Performing the angular integration in (60) we get the photon energy spectrum

$$d\sigma_0^{(ISR)} = \frac{2\alpha^3}{s} \frac{1}{1-x} \left\{ 2 \left( 1 - x + \frac{x^2}{2} \right) \ln \frac{1 + c_m}{1 - c_m} - c_m x^2 \right\} \frac{dx}{x}, \quad (61)$$

where the photon energy fraction  $x = \omega/E$  and  $E$  is the CMS beam energy. Also,  $c_m = \cos \theta_{min}$  represents the angular cut on the photon. Note that

$$1 + \frac{s'^2}{s^2} = 2 - 2x + x^2.$$

The distribution (61) is generated as follows. As the first step, preliminary distribution (the norm is not included)

$$p_0(x) = \frac{1}{x(1-x)}$$

is generated by analytic inversion. Then the acceptance-rejection method is applied with the weight

$$w = 2 \left( 1 - x + \frac{x^2}{2} \right) \ln \frac{1 + c_m}{1 - c_m} - c_m x^2.$$

The photon energy fraction  $x$  is generated in this way in the interval  $x_{min} \leq x \leq x_{max}$ , where

$$x_{max} = 1 - \frac{m_\mu^2}{E^2}.$$

Now we need to generate angular variables for the photon. The matrix element does not depend on the photon azimuthal angle. So this angle  $0 \leq \phi \leq 2\pi$  is generated as an uniform distribution. For the polar angle, Eq. (60) shows that we need to generate the distribution

$$f(\cos \theta) = \frac{1}{1 - \cos^2 \theta} - \frac{x^2}{2(2 - 2x + x^2)}.$$

Again, we use the analytic inversion method to generate the first term of this distribution, which is peaked at small angles, and then acceptance-rejection is applied with weights

$$1 - \frac{x^2(1 - \cos^2 \theta)}{2(2 - 2x + x^2)}.$$

The photon polar angle is restricted to the interval  $-c_m \leq \cos \theta \leq c_m$ .

To generate the muon momentum, let us note that

$$\int \delta(Q - q_- - q_+) \frac{d\vec{q}_-}{E_-} \frac{d\vec{q}_+}{E_+} = \frac{\beta^*}{2} \int d\cos \theta_-^* d\phi_-^*,$$

where  $\theta_-^*$  and  $\phi_-^*$  are  $\mu^-$  angular variables in the dimuon rest frame. As  $R_0^{(ISR)}$  does not depend on these variables,  $\cos \theta_-^*$  and  $\phi_-^*$  are generated as uniform distributions and then  $\mu^-$  four-momentum can be constructed simply in the dimuon rest frame. Finally, we apply Lorentz transformation to transform this four-momentum back to the CMS frame.

The total crude ISR cross section is found by integrating (61):

$$\begin{aligned} \sigma_0^{(ISR)} = & \frac{2\alpha^3}{s} \left[ 2 \ln \frac{x_{max}}{x_{min}} \ln \frac{1 + c_m}{1 - c_m} + \right. \\ & \left. + \left( \ln \frac{1 + c_m}{1 - c_m} - c_m \right) \left( \ln \frac{1 - x_{min}}{1 - x_{max}} - x_{max} + x_{min} \right) \right]. \end{aligned} \quad (62)$$

### 4.3 Crude distribution for the final state radiation

As a crude distribution which models peculiarities of the final state radiation according to (49), we take (the role of  $s$  is to obtain the correct dimension):

$$R_0^{(FSR)} = \frac{s}{y_1 y_2}. \quad (63)$$

Note that

$$y_1 + y_2 = k \cdot (p_+ + p_-) = 2E(2E - E_+ - E_-) \quad (64)$$

and

$$y_1 - y_2 = (q_+ - q_-) \cdot (q_+ + q_- + k) = 2E(E_+ - E_-).$$

These two relations enable us to find

$$y_1 = 2E(2E - E_-), \quad y_2 = 2E(2E - E_+). \quad (65)$$

Now let us transform the phase space

$$\int \delta(Q - q_- - q_+) \frac{d\vec{q}_-}{E_-} \frac{d\vec{q}_+}{E_+} \frac{d\vec{k}}{\omega} = \int d\omega \, d\phi_+^\gamma \frac{dy_2}{2E} d\cos\theta_+ \, d\phi_+,$$

where  $\theta_+$ ,  $\phi_+$  are  $\mu^+$  angular variables and the photon angles  $\theta_+^\gamma$ ,  $\phi_+^\gamma$  are defined with respect to the  $\mu^+$  momentum  $\vec{q}_+$  (the photon polar angle  $\theta_+^\gamma$  does not appear in the r.h.s. of the above formula because energy  $\delta$ -function enables to integrate over  $d\cos\theta_+^\gamma$ ). Therefore the crude distribution for final state radiation takes the form

$$d\sigma_0^{(FSR)} = \frac{\alpha^3}{8\pi^2} \frac{1}{2E y_1 y_2} d\omega \, d\phi_+^\gamma \, dy_2 \, d\cos\theta_+ \, d\phi_+.$$

It is clear that  $\phi_+^\gamma$ ,  $\phi_+$  and  $\cos\theta_+$  are distributed uniformly. Integrating over them and using

$$\frac{1}{y_1 y_2} = \frac{1}{2E\omega} \left( \frac{1}{y_1} + \frac{1}{y_2} \right),$$

we get  $d\sigma_0^{(FSR)}$  as a sum of two distributions

$$d\sigma_0^{(FSR)} = \frac{\alpha^3}{s} \frac{d\omega}{\omega} \frac{dy_1}{y_1} + \frac{\alpha^3}{s} \frac{d\omega}{\omega} \frac{dy_2}{y_2}, \quad (66)$$

where we have also used  $|dy_2| = |dy_1|$  for fixed  $\omega$  as follows from Eq. (64). Integration limits on  $y_1$  and  $y_2$  are determined in the following way. From

$$2E - \omega - E_+ = E_- = \sqrt{\omega^2 + E_+^2 + 2\omega|\vec{q}_+| \cos\theta_+^\gamma}$$

we find

$$\cos\theta_+^\gamma = \frac{2E(E - \omega) - E_+(2E - \omega)}{\omega \sqrt{E_+^2 - m_\mu^2}}. \quad (67)$$

Since  $|\cos\theta_+^\gamma| \leq 1$ , we find allowed region for  $E_+$ :

$$\frac{1}{2} \left[ 2 - x - x\sqrt{1 - \frac{\mu^2}{1-x}} \right] \leq x_+ \leq \frac{1}{2} \left[ 2 - x + x\sqrt{1 - \frac{\mu^2}{1-x}} \right],$$

where  $x_+ = E_+/E$  and  $\mu = m_\mu/E$ . Using now  $y_2 = 2E^2(1 - x_+)$ , we derive

$$x \left[ 1 - \sqrt{1 - \frac{\mu^2}{1-x}} \right] \leq \frac{y_2}{E^2} \leq x \left[ 1 + \sqrt{1 - \frac{\mu^2}{1-x}} \right]. \quad (68)$$

The limits for  $y_1$  are the same as  $y_1 = 2E^2x - y_2$  relation shows. Therefore, integrating (66) over  $y_{1,2}$ , we get the following photon energy spectrum

$$d\sigma_0^{(FSR)} = \frac{2\alpha^3}{s} \ln \frac{\sqrt{1-x} + \sqrt{1-x-\mu^2}}{\sqrt{1-x} - \sqrt{1-x-\mu^2}} \frac{dx}{x}. \quad (69)$$

Using this distribution, we can generate the photon energy in the following way. Noting that

$$\ln \frac{\sqrt{1-x} + \sqrt{1-x-\mu^2}}{\sqrt{1-x} - \sqrt{1-x-\mu^2}} \rightarrow \frac{\ln(1-x)}{x} + \frac{\ln(s/m_\mu^2)}{x},$$

when  $\mu \rightarrow 0$ , we first generate the distribution (the norm is not included)

$$p_0(x) = \frac{\ln(1-x)}{x} + \frac{\ln(s/m_\mu^2)}{x}$$

by numerically solving the equation

$$r = \ln\left(\frac{s}{m_\mu^2}\right) \ln\left(\frac{x}{x_{min}}\right) + \text{Li}_2(x_{min}) - \text{Li}_2(x),$$

where  $r$  is a random number uniformly distributed in the interval

$$0 \leq r \leq \ln\left(\frac{s}{m_\mu^2}\right) \ln\left(\frac{x_{max}}{x_{min}}\right) + \text{Li}_2(x_{min}) - \text{Li}_2(x_{max}).$$

Then the desired distribution (69) is reproduced by the acceptance-rejection method with the weight

$$w = \ln \frac{2(1-x) - \mu^2 + 2\sqrt{(1-x)(1-x-\mu^2)}}{\mu^2} \bigg/ \ln \frac{4(1-x)}{\mu^2}.$$

After the photon energy is generated, we can generate  $\mu^+$ -energy as well. First  $1/y$  distribution is generated by analytic inversion. Then we generate a random number  $r$  uniformly distributed in the interval  $0 \leq r \leq 1$  and if  $r \leq 0.5$  we take  $y_1 = y$ , otherwise we take  $y_2 = y$ , which means that we choose between two sub-distributions in (66). Knowing  $y_1$  or  $y_2$  allows us to determine  $E_+$  from (65) and energy conservation.

As we mentioned earlier,  $\phi_+^\gamma$ ,  $\phi_+$  and  $\cos\theta_+$  are generated as uniform distributions and  $\cos\theta_+^\gamma$  is determined by (67). The only thing which is left is to rotate generated three-momentum of the photon correctly, because  $\cos\theta_+^\gamma$  and  $\phi_+^\gamma$  determine its orientation with respect to  $\mu^+$ -momentum  $\vec{q}_+$ , but not with respect to our initial CMS axes. Note that this  $q_+$ -reference frame can be obtained from the initial  $p_-$ -reference frame (in which  $\vec{p}_-$  points along  $z$ -direction) by two consecutive rotations: rotation by the angle  $\phi_+$  around  $z$ -th axis followed by rotation around the new  $y$  axis by the angle  $\theta_+$ . This allows us to construct the transformation law for any vector  $\vec{A} = \{A_x, A_y, A_z\}$  under the combined rotation:

$$\begin{aligned} A_x &= \cos\theta_+ \cos\phi_+ A'_x - \sin\phi_+ A'_y + \sin\theta_+ \cos\phi_+ A'_z, \\ A_y &= \cos\theta_+ \sin\phi_+ A'_x + \cos\phi_+ A'_y + \sin\theta_+ \sin\phi_+ A'_z, \\ A_z &= -\sin\theta_+ A'_x + \cos\theta_+ A'_z, \end{aligned} \quad (70)$$

where  $\{A'_x, A'_y, A'_z\}$  and  $\{A_x, A_y, A_z\}$  are the vector coordinates in the  $q_+$ -reference frame and the desired coordinates in the  $p_-$ -reference frame, respectively. All what is needed to complete the generation of the photon momentum is to apply (70) to the case  $\vec{A} = \vec{k}$  and use

$$k'_x = \omega \sin\theta_+^\gamma \cos\phi_+^\gamma, \quad k'_y = \omega \sin\theta_+^\gamma \sin\phi_+^\gamma, \quad k'_z = \omega \cos\theta_+^\gamma.$$

After the FSR event is generated with crude distribution, it is only accepted if the photon polar angle is in the interval  $-c_m \leq \cos \theta \leq c_m$ . Otherwise the procedure is repeated.

We also need the total crude FSR cross section. It can be obtained by integrating (69), but there is some subtlety in how to account for the photon angular cut. Note that

$$\int \frac{1}{y_1 y_2} \delta(p_- + p_+ - k - q_- - q_+) \frac{d\vec{q}_-}{E_-} \frac{d\vec{q}_+}{E_+}$$

can depend only on  $k \cdot (p_- + p_+)$  and not separately on  $k \cdot p_-$  and/or  $k \cdot p_+$ . Therefore in the CMS frame  $d\sigma_0^{(FSR)}/d\vec{k}$  does not depend on the photon angular variables. Hence the distribution over  $\cos \theta$  is uniform and the desired total cross section is given by:

$$\sigma_0^{(FSR)} = \frac{2\alpha^3 c_m}{s} \int_{x_{min}}^{1-\mu^2} \ln \frac{2(1-x) - \mu^2 + 2\sqrt{(1-x)(1-x-\mu^2)}}{\mu^2} \frac{dx}{x}. \quad (71)$$

This integral is calculated numerically in the MUMUG program.

## 5 Concluding remarks

In the present paper, we have described and made available MUMUG, a new leading-order Monte Carlo program that simulates  $e^+e^- \rightarrow \mu^+\mu^-\gamma$  process.

We hope that the MUMUG program in conjunction with this article can be used for educational purposes. Therefore, we have presented a very detailed description of the Monte Carlo algorithm used, as well as the helicity amplitude method and the calculation of the  $e^+e^- \rightarrow \mu^+\mu^-\gamma$  matrix element by means of this method.

For reference purposes, in Table 1 we provide some total cross sections calculated by using the MUMUG program. For comparison with other programs, keep in mind that professional Monte Carlo programs such as AFKQED or MCGPJ include the emission of additional collinear photons, while others, such as PHOKHARA and KKMC, include next-to-leading order radiative corrections. All these improvements are missing in the MUMUG generator.

$\omega_{min} \backslash \theta_{min}$	10°	15°	20°	25°
0.1 GeV	206.20 ± 0.18	182.83 ± 0.16	164.60 ± 0.14	149.24 ± 0.13
0.15 GeV	187.54 ± 0.16	165.62 ± 0.14	148.70 ± 0.13	134.43 ± 0.12
0.20 GeV	174.35 ± 0.15	153.43 ± 0.13	137.56 ± 0.12	124.08 ± 0.11
0.25 GeV	164.28 ± 0.14	143.99 ± 0.12	128.86 ± 0.11	116.14 ± 0.10

**Table 1** The total cross sections of  $e^+e^- \rightarrow \mu^+\mu^-\gamma$  in picobarns for the CMS beam energy  $E = 5.29$  GeV and for different values of the minimum photon energy ( $\omega_{min}$ ) and angular cuts imposed on the photon polar angle ( $\theta_{min}$ ).

The Fortran code of the MUMUG program can be downloaded (under the MIT license) from: <https://wwwsnd.inp.nsk.su/~silagadz/MUMUG/>, or from the Code Ocean Capsule: <https://codeocean.com/capsule/4243841/tree/v1>.

**Acknowledgements** The work is supported by the Ministry of Education and Science of the Russian Federation and in part by RFBR grant 20-02-00697-a.

## Appendix

### A Feynman rules used in the main text

Each Feynman diagram determines a contribution to the momentum space matrix element of the process under consideration. This contribution can be found from the diagram according to the following rules (only ones relevant for our studies are listed). Their derivations can be found in the standard quantum field theory textbooks [29].

- Initial state particles with 4-momentum  $p$ :

$$\text{electron} \quad \text{---} \rightarrow \bullet \quad u_\lambda(p)$$

$$\text{positron} \quad \leftarrow \text{---} \bullet \quad \bar{v}_\lambda(p)$$

where  $\lambda$  stands for the fermion polarization.  $u_\lambda(p)$  and  $v_\lambda(p)$  are particle and antiparticle Dirac spinors.

- Final state particles with 4-momentum  $p$ :

$$\text{electron} \quad \bullet \rightarrow \text{---} \quad \bar{u}_\lambda(p)$$

$$\text{positron} \quad \bullet \leftarrow \text{---} \quad v_\lambda(p)$$

$$\text{photon} \quad \bullet \text{---} \text{---} \bullet \quad \epsilon_\mu^*(p)$$

$\epsilon_\mu$  is the photon polarization four-vector.

- Intermediate state particle propagators with 4-momentum  $p$ :

$$\text{fermion} \quad \bullet \text{---} \bullet \quad \frac{i(\not{p} + m)}{p^2 - m^2 + i\epsilon}$$

$$\text{photon} \quad \bullet \text{---} \bullet \quad \frac{-ig_{\mu\nu}}{p^2 + i\epsilon}$$

- Interaction vertex:

$$\begin{array}{c} \swarrow \\ \bullet \\ \searrow \end{array} \text{---} \text{---} \quad -ie\gamma_\mu$$

### B Usage of the program

To generate pseudorandom numbers uniformly distributed in the interval  $(0, 1)$ , the program uses *RANLUX* generator from the CERNLIB library [41]. Therefore, if the user does not want to use default values for *RANLUX*, *RLUXGO* subroutine should be called to initialize *RANLUX*, as described in [41].

Various internal common blocks of MUMUG are filled when

$$FILCOM(E, EGMIN, THGMIN)$$

subroutine is called. Here  $E(REAL*8)$  is the CMS beam energy in GeV.  $EGMIN(REAL*8)$  represents the minimum energy of the photon, also in GeV, and  $THGMIN(REAL*8)$  is the angular cut on the photon polar angle in degrees.

After *RANLUX* generator was initialized, and *FILCOM* subroutine was called, MUMUG is ready to generate events of the process  $e^+e^- \rightarrow \mu^+\mu^-\gamma$ . Each call of the

$$MUMUG(E, QM, QP, K, IMOD)$$

subroutine results in the output of  $REAL * 8$  arrays  $QM(0 : 3)$ ,  $QP(0 : 3)$ ,  $K(0 : 3)$ , which represent four-momenta of the produced particles ( $\mu^+$ ,  $\mu^-$  and  $\gamma$ , respectively).

The  $IMOD(INTEGER)$  parameter specifies which expression is used by MUMUG when calculating the matrix element of  $e^+e^- \rightarrow \mu^+\mu^-\gamma$  (or its modulus squared). In particular, if  $IMOD = 0$ , expression (12) (with the corrected sign misprint) from [8] is used. If  $IMOD = 1$ , expressions (9 – 10) from [8] are used. If  $IMOD = 2$ , the results of [35] are used. At last, if  $IMOD = 3$ , our helicity amplitudes, described in this article, are used. These different modes of matrix element calculation have been implemented in MUMUG in order to facilitate the detection of various programming mistakes (bugs) during the program development. All modes produce identical output (within the precision expected by the double precision arithmetic used).

After sufficiently large number of MUMUG calls,  $crs(E, sg, sgerr)$  subroutine, if called, estimates the cross section  $sg(REAL * 8)$  of the process  $e^+e^- \rightarrow \mu^+\mu^-\gamma$ ,  $E_\gamma > EGMIN$ ,  $THGMIN < \theta_\gamma < 180^\circ - THGMIN$ , and its error  $sgerr(REAL * 8)$  in picobarns.

## References

1. A. Bogomyagkov, V. Druzhinin, E. Levichev, A. Milstein and S. Sinyatkin, Low-energy electron-positron collider to search and study  $\mu^+\mu^-$  bound state, EPJ Web Conf. **181** (2018), 01032. <https://doi.org/10.1051/epjconf/201818101032>
2. S. J. Brodsky and R. F. Lebed, Production of the Smallest QED Atom: True Muonium ( $\mu^+\mu^-$ ), Phys. Rev. Lett. **102** (2009), 213401. <https://doi.org/10.1103/PhysRevLett.102.213401>
3. H. Lamm and Y. Ji, Predicting and Discovering True Muonium ( $\mu^+\mu^-$ ), EPJ Web Conf. **181** (2018), 01016. <https://doi.org/10.1051/epjconf/201818101016>
4. A. A. Bajkov, Precision measurement of the CMS energy and its spread at the Muon-muon collider, bachelor's thesis under supervision of V. Druzhinin, Novosibirsk, 2019.
5. N. Amapane *et al.*, Study of muon pair production from positron annihilation at threshold energy, JINST **15** (2020), P01036. <https://doi.org/10.1088/1748-0221/15/01/P01036>
6. E. Barberio, B. van Eijk and Z. Was, PHOTOS: A Universal Monte Carlo for QED radiative corrections in decays, Comput. Phys. Commun. **66** (1991), 115–128. [https://doi.org/10.1016/0010-4655\(91\)90012-A](https://doi.org/10.1016/0010-4655(91)90012-A)
7. E. Barberio and Z. Was, PHOTOS: A Universal Monte Carlo for QED radiative corrections. Version 2.0, Comput. Phys. Commun. **79** (1994), 291–308. [https://doi.org/10.1016/0010-4655\(94\)90074-4](https://doi.org/10.1016/0010-4655(94)90074-4)
8. A. B. Arbuzov *et al.*, Large angle QED processes at  $e^+e^-$  colliders at energies below 3-GeV, JHEP **9710** (1997), 001. <https://doi.org/10.1088/1126-6708/1997/10/001>
9. J. P. Lees *et al.* [BaBar], Measurement of initial-state-final-state radiation interference in the processes  $e^+e^- \rightarrow \mu^+\mu^-\gamma$  and  $e^+e^- \rightarrow \pi^+\pi^-\gamma$ , Phys. Rev. D **92** (2015), 072015. <https://doi.org/10.1103/PhysRevD.92.072015>
10. V. P. Druzhinin, S. I. Eidelman, S. I. Serednyakov and E. P. Solodov, Hadron Production via  $e^+e^-$  Collisions with Initial State Radiation, Rev. Mod. Phys. **83** (2011), 1545–1588. <https://doi.org/10.1103/RevModPhys.83.1545>
11. H. Czyż, A. Grzebińska and E. Nowak-Kubát, Radiative return method as a tool in hadronic physics, Acta Phys. Polon. B **36** (2005), 3403–3412. <https://arxiv.org/abs/hep-ph/0510208>
12. M. Benayoun, S. I. Eidelman, V. N. Ivanchenko and Z. K. Silagadze, Spectroscopy at B factories using hard photon emission, Mod. Phys. Lett. A **14** (1999), 2605–2614. <https://doi.org/10.1142/S021773239900273X>
13. F. Campanario, H. Czyż, J. Gluza, M. Guina, T. Riemann, G. Rodrigo and V. Yundin, Complete QED NLO contributions to the reaction  $e^+e^- \rightarrow \mu^+\mu^-\gamma$  and their implementation in the event generator PHOKHARA, JHEP **02** (2014), 114. [https://doi.org/10.1007/JHEP02\(2014\)114](https://doi.org/10.1007/JHEP02(2014)114)
14. S. Jadach, B. F. L. Ward and Z. Was, The Precision Monte Carlo event generator KK for two fermion final states in  $e^+e^-$  collisions, Comput. Phys. Commun. **130** (2000), 260–325. [https://doi.org/10.1016/S0010-4655\(00\)00048-5](https://doi.org/10.1016/S0010-4655(00)00048-5)
15. S. Jadach, B. F. L. Ward and Z. Was, Coherent exclusive exponentiation for precision Monte Carlo calculations, Phys. Rev. D **63** (2001), 113009. <https://doi.org/10.1103/PhysRevD.63.113009>
16. A. B. Arbuzov, G. V. Fedotov, F. V. Ignatov, E. A. Kuraev and A. L. Sibidanov, Monte-Carlo generator for  $e^+e^-$  annihilation into lepton and hadron pairs with precise radiative corrections, Eur. Phys. J. C **46** (2006), 689–703. <https://doi.org/10.1140/epjc/s2006-02532-8>
17. R. Gastmans and T. T. Wu, *The Ubiquitous Photon: Helicity Methods for QED and QCD* (Clarendon Press: Oxford, 1990).

18. V. F. Dmitriev and A. I. Milstein, Final state Coulomb interaction and asymmetry of pair production close to threshold in  $e^+e^-$  annihilation, Phys. Lett. B **722** (2013), 83–85. <https://doi.org/10.1016/j.physletb.2013.03.036>
19. R. Kleiss and W. J. Stirling, Spinor Techniques For Calculating  $P$  Anti- $P \rightarrow W^\pm / Z^0 + \text{Jets}$ , Nucl. Phys. B **262** (1985), 235–262. [https://doi.org/10.1016/0550-3213\(85\)90285-8](https://doi.org/10.1016/0550-3213(85)90285-8)
20. R. Kleiss and W. J. Stirling, Cross-Sections For The Production Of An Arbitrary Number Of Photons In Electron - Positron Annihilation, Phys. Lett. B **179** (1986), 159–163. [https://doi.org/10.1016/0370-2693\(86\)90454-5](https://doi.org/10.1016/0370-2693(86)90454-5)
21. Z. Xu, D. H. Zhang and L. Chang, Helicity Amplitudes For Multiple Bremsstrahlung In Massless Nonabelian Gauge Theories, Nucl. Phys. B **291** (1987), 392–428. [https://doi.org/10.1016/0550-3213\(87\)90479-2](https://doi.org/10.1016/0550-3213(87)90479-2)
22. S. Jadach, B. F. Ward and Z. Was, Global positioning of spin GPS scheme for half-spin massive spinors, Eur. Phys. J. C **22** (2001), 423–430. <https://doi.org/10.1007/s100520100818>
23. M. L. Mangano and S. J. Parke, Multiparton amplitudes in gauge theories, Phys. Rept. **200** (1991), 301–367. [https://doi.org/10.1016/0370-1573\(91\)90091-Y](https://doi.org/10.1016/0370-1573(91)90091-Y)
24. H. K. Dreiner, H. E. Haber and S. P. Martin, Two-component spinor techniques and Feynman rules for quantum field theory and supersymmetry, Phys. Rept. **494** (2010), 1–196. <https://doi.org/10.1016/j.physrep.2010.05.002>
25. M. E. Peskin, Simplifying Multi-Jet QCD Computation, arXiv:1101.2414 [hep-ph]. <https://arxiv.org/abs/1101.2414>
26. L. J. Dixon, Calculating scattering amplitudes efficiently, arXiv:hep-ph/9601359 [hep-ph]. <https://arxiv.org/abs/hep-ph/9601359>
27. R. K. Ellis, Z. Kunszt, K. Melnikov and G. Zanderighi, One-loop calculations in quantum field theory: from Feynman diagrams to unitarity cuts, Phys. Rept. **518** (2012), 141–250. <https://doi.org/10.1016/j.physrep.2012.01.008>
28. H. Elvang and Y. t. Huang, Scattering Amplitudes, arXiv:1308.1697 [hep-th]. <https://arxiv.org/abs/1308.1697>
29. For example:  
N. N. Bogolyubov and D. V. Shirkov, *Introduction to the Theory of Quantized Fields* (Wiley, 1980.)  
J. D. Bjorken and S. D. Drell, *Relativistic Quantum Fields* (McGraw-Hill, 1965.)  
M. E. Peskin and D. V. Schroeder, *An Introduction to Quantum Field Theory* (Addison-Wesley, 1995.)  
S. Weinberg, *The Quantum Theory of Fields* (Cambridge Univ. Press, 1995.)
30. R. Kleiss and S. van der Marck, Two Photon Bremsstrahlung, Nucl. Phys. B **342** (1990), 61–94. [https://doi.org/10.1016/0550-3213\(90\)90571-T](https://doi.org/10.1016/0550-3213(90)90571-T)
31. A. C. Hearn, *REDUCE User's Manual, version 3.4* (Rand Corporation, Santa Monika, 1993.)
32. M. Martinez, R. Miquel and C. Mana, Helicity Amplitudes Calculation, AIP Conf. Proc. **201** (1990), 243–258. <https://doi.org/10.1063/1.39078>
33. A. Ballestrero, E. Maina and S. Moretti, Heavy quarks and leptons at  $e^+e^-$  colliders, Nucl. Phys. B **415** (1994), 265–292. [https://doi.org/10.1016/0550-3213\(94\)90112-0](https://doi.org/10.1016/0550-3213(94)90112-0)
34. F. A. Berends, R. Kleiss, P. De Causmaecker, R. Gastmans, W. Troost and T. T. Wu, Multiple Bremsstrahlung In Gauge Theories At High-Energies. 2. Single Bremsstrahlung, Nucl. Phys. B **206** (1982), 61–89. [https://doi.org/10.1016/0550-3213\(82\)90489-8](https://doi.org/10.1016/0550-3213(82)90489-8)
35. F. A. Berends, R. Kleiss, S. Jadach and Z. Was, QED Radiative Corrections To Electron - Positron Annihilation Into Heavy Fermions, Acta Phys. Polon. B **14** (1983), 413–424. <https://www.actaphys.uj.edu.pl/R/14/6/413/pdf>
36. S. Weinzierl, Introduction to Monte Carlo methods, hep-ph/0006269. <https://arxiv.org/abs/hep-ph/0006269>
37. S. Jadach, Practical guide to Monte Carlo, physics/9906056. <https://arxiv.org/abs/physics/9906056>
38. F. A. Berends and R. Kleiss, Initial State Radiation For  $e^+e^-$  Annihilation Into Jets, Nucl. Phys. B **178** (1981), 141–150; [https://doi.org/10.1016/0550-3213\(81\)90500-9](https://doi.org/10.1016/0550-3213(81)90500-9)  
F. A. Berends, R. Kleiss and S. Jadach, Radiative Corrections To Muon Pair And Quark Pair Production In Electron - Positron Collisions In The  $Z(0)$  Region, Nucl. Phys. B **202** (1982), 63–88. [https://doi.org/10.1016/0550-3213\(82\)90221-8](https://doi.org/10.1016/0550-3213(82)90221-8)
39. F. A. Berends and R. Kleiss, Distributions In The Process  $e^+e^- \rightarrow \mu^+\mu^-(\gamma)$ , Nucl. Phys. B **177** (1981), 237–262. [https://doi.org/10.1016/0550-3213\(81\)90390-4](https://doi.org/10.1016/0550-3213(81)90390-4)  
See also E. A. Kuraev and G. V. Meledin, QED Distributions For Hard Photon Emission In  $e^+e^- \rightarrow \mu^+\mu^-\gamma$ , Nucl. Phys. B **122** (1977), 485–492. [https://doi.org/10.1016/0550-3213\(77\)90141-9](https://doi.org/10.1016/0550-3213(77)90141-9)
40. F. A. Berends, R. Kleiss and S. Jadach, Monte Carlo Simulation Of Radiative Corrections To The Processes  $e^+e^- \rightarrow \mu^+\mu^-$  And  $e^+e^- \rightarrow \text{Anti-Q} Q$  In The  $Z^0$  Region, Comput. Phys. Commun. **29** (1983), 185–200. [https://doi.org/10.1016/0010-4655\(83\)90073-5](https://doi.org/10.1016/0010-4655(83)90073-5)

- 
41. F. James, V115: Uniform Random Numbers of Guaranteed Quality,  
<http://hep.fi.infn.it/cernlib.pdf> pp. 332-33 (accessed August 19, 2021).